Dual Model with Non-Linear Baryon Trajectories and Pion-Nucleon Backward Scattering

Kikuji Hirose

Abstract

A dual model with the non-linear baryon trajectories is constructed for πN scattering. It is assumed that both the I=3/2 and 1/2 families of πN resonances lie on the non-linear trajectories in the form $\alpha(\sqrt{s})=a+bs+c\sqrt{s}$. However, a well-known quantum mechanical level mixing (a cross-over phenomenon) occurs between the two mutually crossing I=1/2 trajectories and shifts the branch point of $\alpha(\sqrt{s})$ to the region $s<0$. Many difficulties concerning πN backward scattering, so far encountered in the model with linear baryon trajectories, are overcome by virtue of the non-linearity of the baryon trajectories and by the effect of the cross-over phenomenon. Our model gives a reasonable agreement with the experimental data for the backward differential cross-section and polarization, in addition to the good results for low-energy resonance parameters.

§1. Introduction

In the recent several years, the concept of the duality has become to occupy the major part of the theoretical particle physics. The qualitative features of the dual amplitudes give us a better understanding of many basic concepts of the particle physics, i.e., the non-existence of exotic resonances, the exchange degeneracy, the origin of Regge behavior (hadrons may have much more complicated structure than the simple bound states of two elementary particles) and the structure of the hadronic matter, etc. On the other hand, for the quantitative argument one is most interested in that the Veneziano-type amplitudes provide the unified description of both low- and high-energy hadron scattering processes. In πN scattering, where extensive experimental informations are available, many authors[1] have investigated how well a Veneziano-type representation correlates the low-energy resonance parameters with the high-energy data. However it has been pointed out that when adjustable parameters are so determined that the model can reproduce the empirical elastic widths of low-energy πN resonances, the Veneziano-type amplitude leads to the enormously large backward differential cross-sections at high-energy, even if the results for forward region are satisfactory. In order to clarify whether the duality describes only the gross feature of the hadron dynamics or it gives also quantitative completeness of the amplitude of the hadronic process, except for the amplitude concerning the Pomeron-exchange, it is extremely important to proceed detailed and more careful investigations for this problem.

In all the previous investigations, it was assumed that all of baryons as well as mesons lie on <u>linear</u> trajectories. Since the results predicted by Veneziano-type amplitudes depend entirely on how

we choose the trajectories of many hadrons, we must be very careful in assigning hadron trajectories; especially, the choice of the baryon trajectories is important. The baryon trajectories have features not shared by the case of mesons, an example of which is the MacDowell symmetry.[2] This symmetry asserts that the baryon trajectories must appear as pairs of those with opposite parity and the same signature, and that two trajectory-functions of each pairs define a single analytic function $\alpha(W)$, for which we get $\alpha_{\tau\cdot P=+1}(W)=\alpha(W)$ and $\alpha_{\tau\cdot P=-1}(W)=\alpha(-W)$, where W is c.m. energy of πN scattering, and τ and P stand for the signature and the parity, respectively. Therefore, if we assume the linear trajectory, which is a even function of W, then we obtain degenerate parity doublet, i.e., the doublet consisting of two states with opposite parity, the same spin and equal masses. For the I=1/2 πN resonances, we have seen good examples of this degenerate parity doublets.[3] But we have no examples for I=3/2 states at present. This is the point that we should call attention to.

So far many investigations mentioned above were carried out under the degenerate parity doublets scheme (the linear trajectories) with the elimination of unwanted low-mass parity partners. This is equivalent to the guess that the non-existence of the degenerate parity doublet in low-mass I=3/2 states will be accidental and for higher mass-levels, we shall have such parity doublets. We emphasize another possible viewpoint[4] that the non-existence of the degenerate parity doublets is a common feature of I=3/2 states, at least of the states on the Δ_δ trajectory, i.e., all of the P_{33} (1236) and its higher mass-level states. In this paper we take this point of view. Indeed, we get the following preferable prospects with this scheme.

This viewpoint naturally leads us to conjecture that the I=3/2 states lie on non-linear trajectories which are not even functions of

W and these states form non-degenerate parity doublets. As a candidate for the non-degenerate parity partner of the $P_{33}(1236)$, we take the well-established $J^P=3/2^-$ resonance, the $D_{33}(1670)$. For such non-linear trajectory of $(\Delta_\delta-\Delta_\gamma)$, we get the lower intercept than that of the linear case. This might have effects of suppressing πN backward cross-sections, for which one so far obtained too large predicted values.

For I=1/2 πN resonances, there are the examples of the degenerate parity doublets; say, $F_{15}(1688)$ and $D_{15}(1670)$, etc. However,it is well-known that the observed F/D ratios of these two states are quite different, when we consider these states as members of SU(3) multiplets, and it was difficult to interprete this fact by using linear I=1/2 trajectories.[5] In order to solve this problem, we start from the conjecture that the I=1/2 trajectories also take the non-linear forms, as those in the I=3/2 case. The above mentioned difficulty is readily removed, namely, the degenerate states are no more MacDowell-symmetric pair and are described by two independent trajectory-functions. These two non-linear I=1/2 trajectoties have the same quantum numbers for the unitary spin, isospin and signature, and intersect at W=0. The quantum mechanics tell us that whenever we get two states with nearly equal masses and with the same quantum numbers, a certain level mixing may happen.[6,7] [Hereafter we call it the cross-over phenomenon.] In our case, this happens in the unphysical region (W=0) and the level mixing will be treated by the Gribov Reggeon perturbation theory.[8] The above mentioned non-linear I=1/2 trajectories correspond to the unperturbed trajectories. On the other hand, we shall see in the text that the perturbed trajectories give the result that the degenerate states become again the MacDowell-symmetric pairs, but these have the different F/D ratios.

In this paper, we deal with the construction of the Veneziano-type amplitude for πN scattering which incorporates the non-linear baryon trajectories with the cross-over phenomenon. This must be carried out carefully, because, in general, the introduction of the non-linear trajectories leads to the occurence of the ancestor poles. We shall show that the amplitude without ancestor poles is indeed obtained and that the many problems pointed out are resolved by the use of the non-linear trajectories. Thus, we get better understanding of the duality in the quantitative argument of the hadronic process.

In §2 we develop the general formulation of the cross-over phenomenon for Regge trajectories by employing the Gribov Reggeon calculus.[8] The assignment of the non-linear baryon trajectories will be also given in this section. In §3 we construct the dual representation with a single unperturbed baryon trajectory in the form $a+bW^2+cW$. This is done in the line of thought of Volkov and Radchenko,[9] who gave the first attempt in this direction. In §4 we give the general amplitude which contains many baryon trajectories on the basis of the unperturbed dual representation obtained in §3. In §5 we show that the unperturbed amplitude is easily extended to the perturbed one according to the some simple rule. Thus we get the final form of our dual amplitude for πN scattering. In §6 we deal with the numerical evaluation of the model and the prediction as to high-energy scattering. The final remarks will be given in §7.

§2. Non-linear Regge trajectories of πN resonances and the cross-over phenomenon in I=1/2 trajectories

Before discussing the cross-over phenomenon, we shall determine the unperturbed non-linear baryon trajectories in the very simple form, i.e., $a+bW^2+cW$.

(I=3/2 baryon trajectories)

As already discussed in the introduction, we choose the $D_{33}(1670)$ state as the MacDowell parity partner of the $P_{33}(1236)$. Then we obtain

$$\alpha_\Delta(W)=a_\Delta+b_\Delta W^2+c_\Delta W,$$

$$a_\Delta=-0.30, \quad b_\Delta=0.85\ \mathrm{GeV}^{-2}, \quad c_\Delta=-0.36\ \mathrm{GeV}^{-1}. \qquad (2.1)$$

Here and hereafter we adopt the convention that positive values of W define the trajectory with positive natural parity, $\tau\cdot P=+1$. That is, in this case

$$\alpha_\Delta(W)=\alpha_{\Delta_\gamma}(W), \quad (W\geq 0)$$
$$\alpha_\Delta(-W)=\alpha_{\Delta_\delta}(W), \qquad (2.2)$$

where the function $\alpha_{\Delta_\gamma}(\alpha_{\Delta_\delta})$ denotes the $\Delta_\gamma(\Delta_\delta)$ trajectory. In Fig. 1 and 2, we show the Δ_γ-Δ_δ trajectory.

Fig. 1 Fig. 2

The coefficient c_Δ in (2.1) is not determined unambiguously, and has been so determined that the smallest intercept is obtained for the Δ_γ-Δ_δ trajectory under the condition that the empirical resonance masses are reproduced within two percent errors. Its intercept -0.3 $(=\alpha_\Delta(0))$ is considerably lower than $+0.1$ of the conventional linear Δ_δ trajectory.

(I=1/2 baryon trajectories)

The observed almost degenerate pairs are the $D_{15}(1670)$-$F_{15}(1688)$ and $P_{11}(1470)$-$S_{11}(1535)$. The former pair has very different F/D ratios, i.e., $(F/D)_{D_{15}} \simeq -0.2$ and $(F/D)_{F_{15}} \simeq 0.8$. [5] According to the scheme discussed in the introduction, we assume the following unperturbed non-linear $I=\frac{1}{2}$ trajectories: The conventional N_α and N_β' trajectories are MacDowell-symmetric and are expressed by the single function

$$\alpha_{N_1}(W) = a_N + b_N W^2 + c_N W \ , \qquad (2.3)$$

while the N_α' -N_β trajectory is given by

$$\alpha_{N_2}(W) = a_N + b_N W^2 - c_N W \ , \qquad (2.4)$$

with the same coefficients as those of (2.3). This is due to the approximate degeneracies of $F_{15}(1688)$ on N_α and $D_{15}(1670)$ on N_β and also of $P_{11}(1470)$ on N_α' and $S_{11}(1535)$ on N_β' . [See Fig.3.] Empirically we have

$$a_N = -0.67, \quad b_N = 0.83 \ \text{GeV}^{-2} \text{ and } c_N = 0.40 \ \text{GeV}^{-1}. \qquad (2.5)$$

When we consider the trajectories as the functions of $s(\equiv W^2)$, the MacDowell symmetry is exhibited between the upper and lower branches of the curve in Fig.4. The degeneracy of the F_{15} and D_{15} states is not due to the MacDowell symmetry. These lie on the different trajectories. Thus we can understand without difficulty the large difference between the F/D ratios of the F_{15} and D_{15} states.

Fig. 3 Fig. 4

There exists the well-established $J^P = 3/2^-$ state, the $D_{13}(1520)$. This state lies on the N_γ trajectory whose intercept is -1.13; this value is considerably lower than -0.67 of the above-mentioned N trajectories. Throughout this paper, we shall ignore the N_γ trajectory, since this gives only a small effect on πN backward scattering. [11]

It is important to notice that the $N_\alpha - N_\beta'$ and $N_\alpha' - N_\beta$ trajectories have the same quantum numbers (unitary spin, isospin and signature) and they cross each other at W=0, as seen in Fig. 3. In such a case generally occurs the cross-over phenomenon which is analogous to the well-known quantum level mixing [see Fig. 5]. Indeed an example of this phenomenon for Regge trajectories has been seen in the model calculation of Regge trajectories employing the Bethe-Salpeter equation.[7)]

Fig. 5

Now let us develop the general but simple formulation of the quantum transitions between the two trajectories as a perturbation in the Gribov Reggeon calculus[8)] : Sum up the contribution from all the diagrams in which these two trajectories are successively mixed through the transition vertex g, as shown in Fig. 6.

Fig. 6

Then crossed-channel Froissart-Gribov amplitude f_J can be written as

$$f_J = \left[\frac{g_1^2}{J-\alpha_{N_1}} + \frac{g_2^2}{J-\alpha_{N_2}}\right] + \left[\frac{g_1}{J-\alpha_{N_1}} g \frac{g_2}{J-\alpha_{N_2}} + \frac{g_2}{J-\alpha_{N_2}} g \frac{g_1}{J-\alpha_{N_1}}\right] + \cdots\cdots , \tag{2.6}$$

where g_i's are the particle-Reggeon coupling verteces. Introducing the spinor,

$$\psi = \begin{pmatrix} g_1 \\ g_2 \end{pmatrix}, \tag{2.7}$$

and the 2×2 matrices,

$$D = \begin{pmatrix} \frac{1}{J-\alpha_{N_1}} & 0 \\ 0 & \frac{1}{J-\alpha_{N_2}} \end{pmatrix} \quad \text{and} \quad G = \begin{pmatrix} 0 & g \\ g & 0 \end{pmatrix}, \tag{2.8}$$

we rewrite (2.6) as

$$\begin{aligned} f_J \equiv \psi^T \mathcal{D} \psi &= \psi^T D \psi + \psi^T D G D \psi + \psi^T D G D G D \psi + \cdots\cdots \\ &= \psi^T [D + D G \mathcal{D}] \psi . \end{aligned} \tag{2.9}$$

Hence,

$$\mathcal{D} = D + DG\mathcal{D}. \tag{2.10}$$

From (2.10) we obtain

$$\mathcal{D}^{-1} = D^{-1} - G = \begin{pmatrix} J & 0 \\ 0 & J \end{pmatrix} - \begin{pmatrix} \alpha_{N_1} & g \\ g & \alpha_{N_2} \end{pmatrix}. \tag{2.11}$$

Diagonalizing the matrix $\begin{pmatrix} \alpha_{N_1} & g \\ g & \alpha_{N_2} \end{pmatrix}$, one finds that the perturbed J-plane singularities of the f_J amplitude are

$$J = \frac{\alpha_{N_1} + \alpha_{N_2}}{2} \pm \sqrt{\left(\frac{\alpha_{N_1} - \alpha_{N_2}}{2}\right)^2 + g^2}. \tag{2.12}$$

Applying this results to our $I=\frac{1}{2}$ case, we obtain the two perturbed trajectories

$$\alpha_N^I(W^2) = a_N + b_N W^2 + \sqrt{(c_N W)^2 + g^2}, \tag{2.13a}$$

$$\alpha_N^{II}(W^2) = a_N + b_N W^2 - \sqrt{(c_N W)^2 + g^2}. \tag{2.13b}$$

The functions α_N^I and α_N^{II} correspond to the two branches of the r.h.s. of (2.12). An important fact is that the r.h.s. of (2.13a) and (2.13b) are the even function of W. [Here we have assumed that g is a constant at least approximately.] Thus, for the perturbed trajectories, the MacDowell symmetry is exhibited between the N_α and N_β or the $N_{\alpha'}$ and $N_{\beta'}$ [see Fig.5], which is the same as the conventional scheme. However, in our case, the N_α and N_β trajectories have quite different residue structures, since the perturbation does not affect so much on these structures. This will be shown in §5.

We take the cuts parallel to the imaginary axis, as shown in Fig7. In Fig.8 we show schematically the Chew-Frautschi plot of the four perturbed trajectories, N_α, N_β, $N_{\alpha'}$ and $N_{\beta'}$, all of which are connected analytically with each other.

Fig. 7

Fig. 8

Finally we fix the value of the unknown constant g. A famous dip structure is observed at $u \simeq -0.15$ $(\mathrm{GeV}/c)^2$ in high-energy $\pi^+ p$ backward scattering,[10] and this is usually attributed to the zero of the Regge amplitude at the wrong-signature nonsense point of the nucleon trajectory.[11] We assume that the same situation holds in our model. Then we put

$$\alpha_N^I(-0.15) = -1/2, \tag{2.14}$$

and get

$$g = 0.34. \tag{2.15}$$

§3. Construction of the dual amplitude with a single unperturbed baryon trajectory

In this section, we shall construct the basic representation of the dual amplitude only in terms of a single unperturbed baryon trajectory function,

$$\alpha(W)=a+bW^2+cW. \tag{3.1}$$

In §5, the representation obtained in this section will be extended to the more complicated perturbed case.

We start from the review of the dual amplitude with the conventional linear baryon trajectory (c=0).[1] The invariant matrix amplitude T for πN scattering,*)

$$T(p_2,q_2;p_1,q_1) \equiv A(s,t,u)+\not{q}B(s,t,u), \tag{3.2}$$

is given by the linear combination of the contributions from the many kind of the baryon trajectories, each of which is expressed in terms of the beta-functions as

$$\begin{aligned}&\left\{xB(\tfrac{1}{2}-\alpha(s),\ 1-\alpha_M(t)) + \tilde{x}\not{q}B(\tfrac{1}{2}-\alpha(s),\ 1-\alpha_M(t))\right\}\\ &+\left\{yB(1-\alpha_M(t),\ \tfrac{1}{2}-\alpha(u)) + \tilde{y}\not{q}B(1-\alpha_M(t),\ \tfrac{1}{2}-\alpha(u))\right\}\\ &+\left\{zB(\tfrac{1}{2}-\alpha(s),\ \tfrac{1}{2}-\alpha(u)) + \tilde{z}\not{q}B(\tfrac{1}{2}-\alpha(s),\ \tfrac{1}{2}-\alpha(u))\right\},\end{aligned} \tag{3.3}$$

where $\alpha(x)$ and $\alpha_M(x)$ denote the baryon and meson trajectories, respectively, and have the form $a+bx$ [x=s,t and u]; x,$\tilde{x}$,y,$\tilde{y}$,z and $\tilde{z}$ are multiplicative constants.**) The other notations for the kinematic variables are the following:

---

*) For the sake of simplicity we ignore the isospin here.

**) The crossing properties of the T amplitude can be easily satisfied by the choice of these constants.

$p_1(p_2)$: initial (final) nucleon momentum,

$q_1(q_2)$: initial (final) pion momentum,

$s=(p_1+q_1)^2$, $u=(p_1-q_2)^2$, $t=(p_1-p_2)^2$,

$Q=(q_1+q_2)/2$, $\not{Q}=\gamma_\mu Q^\mu=\gamma Q$. (3.4)

The terms in the first, second and third lines in (3.3) will be referred to as the (s-t), (t-u) and (s-u) terms, respectively.

Let us pay attention to the (s-t) term and examine the spin-parity structure of baryon poles in the s-channel. For this purpose we introduce the s-channel parity-definite amplitude, [12]

$$F^{\pm}(\sqrt{s},u)=\mp A(s,t,u)+(\sqrt{s}\pm M)B(s,t,u), \tag{3.5}$$

where M is the mass of the nucleon. Inserting the (s-t) term of (3.3) into the r.h.s. of (3.5), we have

$$F^{+}(\sqrt{s},u)=\sum_{J=1/2}^{\infty}\frac{\Gamma(J-1/2+\alpha_M(t))}{(J-1/2)!\,\Gamma(\alpha_M(t))}\,\frac{-\chi+\tilde{\chi}(\sqrt{s}+M)}{J-\alpha(s)},$$

$$F^{-}(\sqrt{s},u)=\sum_{J=1/2}^{\infty}\frac{\Gamma(J-1/2+\alpha_M(t))}{(J-1/2)!\,\Gamma(\alpha_M(t))}\,\frac{\chi+\tilde{\chi}(\sqrt{s}-M)}{J-\alpha(s)}. \tag{3.6}$$

Here we have used the formula of the beta-function,

$$B(p,q)=\sum_{l=0}^{\infty}\frac{\Gamma(l+1-q)}{l!\,\Gamma(1-q)}\,\frac{1}{l-p}. \tag{3.7}$$

Only the states having the $\tau\cdot P=+1(-1)$ contribute to the $F^+(F^-)$ amplitude.[12] In (3.6) we have the same denominator $(J-\alpha(s))^{-1}$ for both the F^+ and F^-. This means that we have the degenerate MacDowell parity doublets as expected.

The natural extension of (3.6) to the $c\neq 0$ (non-linear) case is obtained as

$$F^{+}(\sqrt{s},u)=\sum_{J=1/2}^{\infty}\frac{\Gamma(J-1/2+\alpha_M(t))}{(J-1/2)!\,\Gamma(\alpha_M(t))}\,\frac{-\chi+\tilde{\chi}(\sqrt{s}+M)}{J-\alpha(\sqrt{s})}\,,$$

$$F^{-}(\sqrt{s},u)=\sum_{J=1/2}^{\infty}\frac{\Gamma(J-1/2+\alpha_M(t))}{(J-1/2)!\,\Gamma(\alpha_M(t))}\,\frac{\chi+\tilde{\chi}(\sqrt{s}-M)}{J-\alpha(-\sqrt{s})}\,. \qquad (3.8)$$

Here we have modified the pole denominators of (3.6) by the non-degenerate MacDowell-symmetric trajectories, $\alpha(\sqrt{s})=a+bs+c\sqrt{s}$ and $\alpha(-\sqrt{s})=a+bs-c\sqrt{s}$. Going back to the beta-functions, we get

$$F^{+}(\sqrt{s},u)=\left[-\chi+\tilde{\chi}(\sqrt{s}+M)\right]\,B(\tfrac{1}{2}-\alpha(\sqrt{s}),\,1-\alpha_M(t)),$$

$$F^{-}(\sqrt{s},u)=\left[\chi+\tilde{\chi}(\sqrt{s}-M)\right]B(\tfrac{1}{2}-\alpha(-\sqrt{s}),\,1-\alpha_M(t)). \qquad (3.9)$$

It is well-known that the non-linear trajectory generally gives rise to the ancestor poles in the crossed-channel, unless the invariant amplitudes are free from the singularity of $\sqrt{s}$ (or $\sqrt{u}$). Now the contribution to the invariant amplitude $T(\equiv A+QB)$ becomes

$$\left[\chi\frac{\sqrt{s}-M-\not{Q}}{2\sqrt{s}}+\tilde{\chi}\,\frac{-s+M^2+(\sqrt{s}+M)\not{Q}}{2\sqrt{s}}\right]B(\tfrac{1}{2}-\alpha(\sqrt{s}),\,1-\alpha_M(t))$$

$$+\left[\chi\frac{\sqrt{s}+M+\not{Q}}{2\sqrt{s}}+\tilde{\chi}\,\frac{s-M^2+(\sqrt{s}-M)\not{Q}}{2\sqrt{s}}\right]B(\tfrac{1}{2}-\alpha(-\sqrt{s}),\,1-\alpha_M(t))\,. \qquad (3.10)$$

This expression is invariant under the transformation $\sqrt{s}\to-\sqrt{s}$, and thus has no branch point at s=0. Accordingly, our amplitude has no ancestor poles.

The expression (3.10) has the following simple integral representation which will be derived in Appendix:

$$\chi B(\tfrac{1}{2}-\alpha_s,\,1-\alpha_M(t))+\tilde{\chi}\tilde{B}(\tfrac{1}{2}-\alpha_s,\,1-\alpha_M(t))\,, \qquad (3.11)$$

and

$$B(x_1,x_2)=\tfrac{1}{2}\int_0^1 dw\left\{w^{x_1-1}(1-w)^{x_2-1}+w^{x_2-1}(1-w)^{x_1-1}\right\},\ ^{*)} \tag{3.12a}$$

$$\tilde{B}(x_1,x_2)=\tfrac{1}{2}\int_0^1 dw\left\{w^{x_1-1}\not{\alpha}_1(1-w)^{x_2-1}+w^{x_2-1}\not{\alpha}_2(1-w)^{x_1-1}\right\}, \tag{3.12b}$$

where $\not{\alpha}_i=\gamma\cdot q_i$ $[i=1,2]$, $\not{\alpha}_s=\gamma\cdot(p_1+q_1)$ and

$$\alpha_s=a+bs-c\not{\alpha}_s. \tag{3.13}$$

The α_s is the matrix in the spinor space, whose eigenvalues represent the non-linear trajectories $\alpha(\pm\sqrt{s})$. The (3.12a) was first derived by Volkov and Radchenko.[9] The expression (3.11) is the generalization of the Volkov-Radchenko amplitude.

The (t-u) and (s-u) terms can be obtained in a similar way, and our final form is

$$\begin{aligned}&\left\{xB(\tfrac{1}{2}-\alpha_s,\ 1-\alpha_M(t))+\tilde{x}\tilde{B}(\tfrac{1}{2}-\alpha_s,\ 1-\alpha_M(t))\right\}\\&+\left\{yB(1-\alpha_M(t),\ \tfrac{1}{2}-\alpha_u)+\tilde{y}\tilde{B}(1-\alpha_M(t),\ \tfrac{1}{2}-\alpha_u)\right\}\\&+\left\{zB(\tfrac{1}{2}-\alpha_s,\ \tfrac{1}{2}-\alpha_u)+\tilde{z}\tilde{B}(\tfrac{1}{2}-\alpha_s,\ \tfrac{1}{2}-\alpha_u)\right\},\end{aligned} \tag{3.14}$$

where

$$\alpha_u=a+bu-c\not{\alpha}_u,\quad \not{\alpha}_u=\gamma\cdot(p_1-q_2). \tag{3.15}$$

The (3.14) possesses correct Regge behavior [cf. (6.2)]. The following crossing properties are also proved:

$$\begin{aligned}&B(\tfrac{1}{2}-\alpha_s,\ 1-\alpha_M(t))\xleftrightarrow{q_1\leftrightarrow -q_2}B(1-\alpha_M(t),\ \tfrac{1}{2}-\alpha_u),\\&\tilde{B}(\tfrac{1}{2}-\alpha_s,\ 1-\alpha_M(t))\xleftrightarrow{q_1\leftrightarrow -q_2}-\tilde{B}(1-\alpha_M(t),\ \tfrac{1}{2}-\alpha_u),\\&B(\tfrac{1}{2}-\alpha_s,\ \tfrac{1}{2}-\alpha_u)\xrightarrow{q_1\leftrightarrow -q_2}B(\tfrac{1}{2}-\alpha_s,\ \tfrac{1}{2}-\alpha_u),\\&\tilde{B}(\tfrac{1}{2}-\alpha_s,\ \tfrac{1}{2}-\alpha_u)\xrightarrow{q_1\leftrightarrow -q_2}-\tilde{B}(\tfrac{1}{2}-\alpha_s,\ \tfrac{1}{2}-\alpha_u).\end{aligned} \tag{3.16}$$

---

*) The function $B(x_1,x_2)$ is nothing but the beta-function, however, the order of the variables $x_{1,2}$ is now important, since these variables are generally the matrices in the spinor space.

§4. The dual amplitude with the three unperturbed baryon trajectories

In this section we shall still deal with the unperturbed baryon trajectories. The basic representation (3.14) obtained in §3 is applied to the three kinds of baryon trajectories, i.e., the Δ_γ-Δ_δ, N_α-N'_β and N'_α-N_β trajectories [see (2.1), (2.3) and (2.4)]. For this purpose, we introduce the matrix trajectory-functions,

$$\begin{aligned}
&\alpha_x^{\Delta} = a_\Delta + b_\Delta x - c_\Delta \nu_x \ , \\
&\alpha_x^{N1} = a_N + b_N x - c_N \nu_x \ , \qquad [x=s,u] \\
&\alpha_x^{N2} = a_N + b_N x + c_N \nu_x \ .
\end{aligned} \tag{4.1}$$

Now the isospin indeces are explicitly written for every quantities. Combining the basic representation (3.14), one obtain the most general expression for the T_I [I=1/2,3/2] amplitudes,

$$\begin{aligned}
T_I(p_2,q_2;p_1,q_1) = &\sum_{\mu=\Delta,N_1,N_2} \left\{ x_I^\mu B(\tfrac{1}{2}-\alpha_s^\mu, 1-\alpha_M(t)) + \tilde{x}_I^\mu \tilde{B}(\tfrac{1}{2}-\alpha_s^\mu, 1-\alpha_M(t)) \right\} \\
&+ \sum_{\mu=\Delta,N_1,N_2} \left\{ y_I^\mu B(1-\alpha_M(t), \tfrac{1}{2}-\alpha_u^\mu) + \tilde{y}_I^\mu \tilde{B}(1-\alpha_M(t), \tfrac{1}{2}-\alpha_u^\mu) \right\} \\
&+ \sum_{\mu,\nu=\Delta,N_1,N_2} \left\{ z_I^{\mu\nu} B(\tfrac{1}{2}-\alpha_s^\mu, \tfrac{1}{2}-\alpha_u^\nu) + \tilde{z}_I^{\mu\nu} \tilde{B}(\tfrac{1}{2}-\alpha_s^\mu, \tfrac{1}{2}-\alpha_u^\nu) \right\} ,
\end{aligned} \tag{4.2}$$

where x_I^μ, $\tilde{x}_I^\mu$, y_I^μ, $\tilde{y}_I^\mu$, $z_I^{\mu\nu}$ and $\tilde{z}_I^{\mu\nu}$ are multiplicative constants. There are 60 constants. However, the crossing symmetry and the elimination of the unwanted baryon states reduce the number of the independent constants to 12.

The crossing relation is

$$T_I(p_2,q_2;p_1,q_1) = \sum_{J=1/2}^{3/2} X_{IJ}\, T_J(p_2,-q_1;p_1,-q_2) \ , \tag{4.3}$$

where $\{X_{IJ}\}$ is the crossing matrix of the isospin[12];

I \ J	1/2	3/2
1/2	-1/3	4/3
3/2	2/3	1/3

(4.4)

Together with the crossing relation (3.16) of the B and $\tilde{B}$ functions, (4.3) leads to the constraints [30 independent relations],

$$x_I^{\mu} = \sum_{J=1/2}^{3/2} X_{IJ}\, y_J^{\mu}\,, \qquad \tilde{x}_I^{\mu} = -\sum_{J=1/2}^{3/2} X_{IJ}\, \tilde{y}_J^{\mu}\,,$$
$$z_I^{\mu\nu} = \sum_{J=1/2}^{3/2} X_{IJ}\, z_J^{\nu\mu}, \qquad \tilde{z}_I^{\mu\nu} = -\sum_{J=1/2}^{3/2} X_{IJ}\, \tilde{z}_J^{\nu\mu}\,. \tag{4.5}$$

Our amplitude (4.2) contains many unwanted baryon states. Unwanted states will be eliminated only on the parent trajectories. For the daughter trajectories, the present experimental knowledge is yet ambiguous so that nothing will be required on the daughters. The residue structure of the parent poles of the amplitudes $F_I^{\pm}$ is found as

$$F_I^{+}(\sqrt{s},u) \simeq \sum_{\mu=\Delta,N_1,N_2} \Big\{ -\Big(x_I^{\mu} + \sum_{\nu=\Delta,N_1,N_2} z_I^{\mu\nu}\Big) + (\sqrt{s}+M)\Big(\tilde{x}_I^{\mu} + \sum_{\nu=\Delta,N_1,N_2} \tilde{z}_I^{\mu\nu}\Big) \Big\}$$
$$\times \sum_{\ell=0}^{\infty} \frac{((-1)^{\ell}+1)}{2\,\ell!}\, \frac{(bu)^{\ell}}{\ell+\frac{1}{2}-\alpha_{\mu}(\sqrt{s})}$$
$$+ \sum_{\mu=\Delta,N_1,N_2} \Big\{ -\Big(x_I^{\mu} - \sum_{\nu=\Delta,N_1,N_2} z_I^{\mu\nu}\Big) + (\sqrt{s}+M)\Big(\tilde{x}_I^{\mu} - \sum_{\nu=\Delta,N_1,N_2} \tilde{z}_I^{\mu\nu}\Big) \Big\}$$
$$\times \sum_{\ell=0}^{\infty} \frac{((-1)^{\ell}-1)}{2\,\ell!}\, \frac{(bu)^{\ell}}{\ell+\frac{1}{2}-\alpha_{\mu}(\sqrt{s})}\,, \tag{4.6a}$$

$$F_I^{-}(\sqrt{s},u) = -F_I^{+}(-\sqrt{s},u)\,, \tag{4.6b}$$

where we have neglected the small difference $b_{\Delta}-b_N$ and put $b \equiv b_{\Delta} = b_N$.

The parent trajectories in (4.6a) are the exchange degenerate type, since the first and the second terms have the same pole denominators but opposite signatures. The observed baryon parent trajectories have the definite signatures [see Fig. 2 and 4], so that we have to eliminate the unwanted states having the wrong signature. The elimination conditions are the following:

(signature condition for the Δ_γ-Δ_δ trajectory)

$$x^{\Delta}_{3/2} + \sum_{\nu=\Delta,N_1,N_2} z^{\Delta\nu}_{3/2} = 0, \quad \widetilde{x^{\Delta}_{3/2}} + \sum_{\nu=\Delta,N_1,N_2} \widetilde{z^{\Delta\nu}_{3/2}} = 0, \tag{4.7}$$

(signature condition for the N_α-N_β and N_α-N_β trajectories)

$$x^{\mu}_{1/2} - \sum_{\nu=\Delta,N_1,N_2} z^{\mu\nu}_{1/2} = 0, \quad \widetilde{x^{\mu}_{1/2}} - \sum_{\nu=\Delta,N_1,N_2} \widetilde{z^{\mu\nu}_{1/2}} = 0. \left[\mu = N_1, N_2\right] \tag{4.8}$$

Furthermore, the multiplicative constants in the r.h.s. of (4.6a) should vanish, whenever the constants relate to the trajectories with the isospin which is not equal to I in the l.h.s. This gives the conditions,

$$x^{\Delta}_{1/2} = \sum_{\nu=\Delta,N_1,N_2} z^{\Delta\nu}_{1/2} = \widetilde{x^{\Delta}_{1/2}} = \sum_{\nu=\Delta,N_1,N_2} \widetilde{z^{\Delta\nu}_{1/2}} = 0, \tag{4.9}$$

$$x^{\mu}_{3/2} = \sum_{\nu=\Delta,N_1,N_2} z^{\mu\nu}_{3/2} = \widetilde{x^{\mu}_{3/2}} = \sum_{\nu=\Delta,N_1,N_2} \widetilde{z^{\mu\nu}_{3/2}} = 0. \left[\mu = N_1, N_2\right] \tag{4.10}$$

Eqs.(4.7)~(4.10) are 18 independent relations; eventually we get totally 12 arbitrary multiplicative constants.

The residue structures of the parent trajectories are now simple: Using (4.7)~(4.10), we get

$$F^{+}_{3/2}(\sqrt{s},u) \simeq -\sum_{\ell=1,3,5,\cdots} \frac{-x^{\Delta}_{3/2} + (\sqrt{s}+M)\widetilde{x^{\Delta}_{3/2}}}{\ell!} \frac{2(bu)^{\ell}}{\ell+\frac{1}{2}-\alpha_{\Delta}(\sqrt{s})}, \tag{4.11a}$$

$$F^{+}_{1/2}(\sqrt{s},u) \simeq \sum_{\ell=0,2,4,\cdots} \frac{-x^{N1}_{\frac{1}{2}}+(\sqrt{s}+M)\widetilde{x^{N1}_{\frac{1}{2}}}}{\ell!} \frac{2(bu)^{\ell}}{\ell+\frac{1}{2}-\alpha_{N1}(\sqrt{s})}$$

$$+ \sum_{\ell=0,2,4,\cdots} \frac{-x^{N2}_{\frac{1}{2}}+(\sqrt{s}+M)\widetilde{x^{N2}_{\frac{1}{2}}}}{\ell!} \frac{2(bu)^{\ell}}{\ell+\frac{1}{2}-\alpha_{N2}(\sqrt{s})} \ . \qquad (4.11b)$$

The six multiplicative constants in the r.h.s. of (4.11) are further restricted, by the crossing relations(4.5), to satisfy the relations

$$x^{\Delta}_{3/2}+x^{N1}_{1/2}+x^{N2}_{1/2}=0 \quad \text{and} \quad -2\widetilde{x^{\Delta}_{3/2}}+\widetilde{x^{N1}_{1/2}}+\widetilde{x^{N2}_{1/2}}=0. \qquad (4.12)$$

For the derivation of these relations, we consider the quantities

$$z_I=\sum_{\mu,\nu=\Delta,N_1,N_2} z_I^{\mu\nu} \quad \text{and} \quad \widetilde{z}_I=\sum_{\mu,\nu=\Delta,N_1,N_2} \widetilde{z_I^{\mu\nu}}. \qquad [I=1/2,3/2] \qquad (4.13)$$

The crossing relations (4.5) become

$$z_I=\sum_{J=1/2}^{3/2} X_{IJ}\, z_J \quad \text{and} \quad \widetilde{z}_I=-\sum_{J=1/2}^{3/2} X_{IJ}\, \widetilde{z}_J \ , \qquad (4.14)$$

and give the solutions

$$z_{1/2}=z_{3/2}, \quad \text{and} \quad \widetilde{z_{1/2}}=-2\widetilde{z}_{3/2} \ . \qquad (4.15)$$

On the other hand, we get from (4.7)~(4.10),

$$z_{1/2}=x^{N1}_{1/2}+x^{N2}_{1/2} \ , \quad z_{3/2}=-x^{\Delta}_{3/2} \ ,$$

$$\widetilde{z}_{1/2}=\widetilde{x^{N1}_{1/2}}+\widetilde{x^{N2}_{1/2}} \quad \text{and} \quad \widetilde{z}_{3/2}=-\widetilde{x^{\Delta}_{3/2}} \ , \qquad (4.16)$$

and inserting these to the both sides of (4.15), we obtain (4.12).

Q.E.D.

The general expression for the elastic widths of the parent resonances can be readily obtained from (4.11);

(for the $\Delta_\gamma, \Delta_\delta$ resonances) $$\Gamma_{ela} = K_R\left\{-x_{3/2}^{\Delta} + (-Pm_R+M)\,\widetilde{x_{3/2}^{\Delta}}\right\}, \qquad (4.17)$$

(for the N_α, N_β' resonances) $$\Gamma_{ela} = K_R\left\{-x_{1/2}^{N1} + (Pm_R+M)\,\widetilde{x_{1/2}^{N1}}\right\}, \qquad (4.18)$$

(for the N_α', N_β resonances) $$\Gamma_{ela} = K_R\left\{-x_{1/2}^{N2} + (Pm_R+M)\,\widetilde{x_{1/2}^{N2}}\right\}, \qquad (4.19)$$

where m_R is the mass of the resonance and

$$K_R = (\tau PE_R - M)\frac{q_R(4bq_R^2)^{J-\frac{1}{2}}}{2\pi b m_R^2}\frac{\Gamma(J+3/2)}{\Gamma(2J+2)} \quad . \qquad (4.20)$$

The nucleon center-of-mass energy and momentum at $\sqrt{s}=m_R$ are denoted by E_R and q_R, respectively. J is the spin of the resonance.

The expression (4.17) for the Δ resonances is our final result. But the (4.18) and (4.19) for the N resonances will be modified further due to the cross-over phenomenon [see the next section]. The elastic widths of all the parent resonances are described by the four adjustable constants. The residual eight adjustable constants are concerned with the widths of the daughter resonances. Since the daughter trajectories give the negligibly small contributions to the high-energy behavior, we will ignore these contributions completely.

§5. The dual amplitude incorporating the cross-over phenomenon

Now the dual amplitude obtained in §4 are easily extended to the perturbed N-trajectories for which the cross-over phenomenon is taken into account. Let us first consider the N-parts of the first term in (4.2); the detailed expression is given by (3.10), i.e.,

$$\sum_{\mu=N_1,N_2}\left[\left\{x_I^{\mu}\frac{\sqrt{s}-M-\not{\alpha}}{2\sqrt{s}}+\tilde{x}_I^{\mu}\frac{-s+M^2+(\sqrt{s}+M)\not{\alpha}}{2\sqrt{s}}\right\}B(\tfrac{1}{2}-\alpha_{\mu}(\sqrt{s}),\ 1-\alpha_M(t))\right.$$
$$\left.+\left\{x_I^{\mu}\frac{\sqrt{s}+M+\not{\alpha}}{2\sqrt{s}}+\tilde{x}_I^{\mu}\frac{s-M^2+(\sqrt{s}-M)\not{\alpha}}{2\sqrt{s}}\right\}B(\tfrac{1}{2}-\alpha_{\mu}(-\sqrt{s}),\ 1-\alpha_M(t))\right]. \quad (5.1)$$

As already emphasized, this expression has no branch point at s=0, although the unperturbed trajectories contain the $\sqrt{s}$ terms. The non-existence of the ancestor poles is due to this situation.

Our perturbed trajectory-functions $\alpha_N^{I,II}(s)$ [(2.13)] contain the term $\sqrt{s+(g/c_N)^2}$. However the invariant amplitudes must have no branch point at $s=-(g/c_N)^2$ for avoiding the ancestor poles. The simplest modification of (5.1) is clearly to replace all the $\sqrt{s}$ terms in (5.1) by the $\sqrt{s+(g/c_N)^2}$. This guarantees the non-existence of the ancestor poles. The result is

$$\left\{x_I^{N1}\frac{\sqrt{s+(g/c_N)^2}-M-\not{\alpha}}{2\sqrt{s+(g/c_N)^2}}+\tilde{x}_I^{N1}\frac{-s+M^2+(\sqrt{s+(g/c_N)^2}+M)\not{\alpha}}{2\sqrt{s+(g/c_N)^2}}\right\}B(\tfrac{1}{2}-\alpha_N^{I}(s),1-\alpha_M(t))$$

$$+\left\{x_I^{N2}\frac{\sqrt{s+(g/c_N)^2}-M-\not{\alpha}}{2\sqrt{s+(g/c_N)^2}}+\tilde{x}_I^{N2}\frac{-s+M^2+(\sqrt{s+(g/c_N)^2}+M)\not{\alpha}}{2\sqrt{s+(g/c_N)^2}}\right\}B(\tfrac{1}{2}-\alpha_N^{II}(s),1-\alpha_M(t))$$

$$+\left\{x_I^{N1}\frac{\sqrt{s+(g/c_N)^2}+M+\not{\alpha}}{2\sqrt{s+(g/c_N)^2}}+\tilde{x}_I^{N1}\frac{s-M^2+(\sqrt{s+(g/c_N)^2}-M)\not{\alpha}}{2\sqrt{s+(g/c_N)^2}}\right\}B(\tfrac{1}{2}-\alpha_N^{II}(s),1-\alpha_M(t))$$

$$+\left\{x_I^{N2}\frac{\sqrt{s+(g/c_N)^2}+M+\not{\alpha}}{2\sqrt{s+(g/c_N)^2}}+\tilde{x}_I^{N2}\frac{s-M^2+(\sqrt{s+(g/c_N)^2}-M)\not{\alpha}}{2\sqrt{s+(g/c_N)^2}}\right\}B(\tfrac{1}{2}-\alpha_N^{I}(s),1-\alpha_M(t)) \ . \quad (5.2)$$

No simple integral representation for (5.2) has been yet found.

The similar procedure is carried out on the other N-terms in (4.2); for the u-channel terms, $\sqrt{u} \longrightarrow \sqrt{u+(g/c_N)^2}$. This gives the final form of our dual πN amplitude. Here we show only the final expression of the elastic widths of the parent N-resonances:

(for the N_α, N_β resonances)

$$\Gamma_{ela}=K_R\left[\tfrac{1}{2}\left(1+\frac{m_R}{\sqrt{m_R^2+(g/c_N)^2}}\right)\left\{-x_{\frac{1}{2}}^{N1}+(Pm_R+M)\widetilde{x_{\frac{1}{2}}^{N1}}\right\}+\tfrac{1}{2}\left(1-\frac{m_R}{\sqrt{m_R^2+(g/c_N)^2}}\right)\left\{-x_{\frac{1}{2}}^{N2}+(Pm_R+M)\widetilde{x_{\frac{1}{2}}^{N2}}\right\}\right], \tag{5.3}$$

(for the N_α', N_β resonances)

$$\Gamma_{ela}=K_R\left[\tfrac{1}{2}\left(1-\frac{m_R}{\sqrt{m_R^2+(g/c_N)^2}}\right)\left\{-x_{\frac{1}{2}}^{N1}+(Pm_R+M)\widetilde{x_{\frac{1}{2}}^{N1}}\right\}+\tfrac{1}{2}\left(1+\frac{m_R}{\sqrt{m_R^2+(g/c_N)^2}}\right)\left\{-x_{\frac{1}{2}}^{N2}+(Pm_R+M)\widetilde{x_{\frac{1}{2}}^{N2}}\right\}\right], \tag{5.4}$$

(for the nucleon pole residue)

$$g_{\pi NN}^2/4\pi=\frac{1}{12\pi bM}\left[\tfrac{1}{2}\left(1+\frac{M}{\sqrt{M^2+(g/c_N)^2}}\right)\left(-x_{\frac{1}{2}}^{N1}+2M\widetilde{x_{\frac{1}{2}}^{N1}}\right)+\tfrac{1}{2}\left(1-\frac{M}{\sqrt{M^2+(g/c_N)^2}}\right)\left(-x_{\frac{1}{2}}^{N2}+2M\widetilde{x_{\frac{1}{2}}^{N2}}\right)\right]. \tag{5.5}$$

The effect of the cross-over phenomenon is evaluated from the factors $\frac{1}{2}\left(1\pm\frac{m_R}{\sqrt{m_R^2+(g/c_N)^2}}\right)$; for the unperturbed case, these take the values $\frac{1}{2}(1\pm1)$. The typical values of these quantities are found for m_R=1500 MeV;

$$\tfrac{1}{2}\left(1+\frac{m_R}{\sqrt{m_R^2+(g/c_N)^2}}\right)\simeq 0.94, \quad \tfrac{1}{2}\left(1-\frac{m_R}{\sqrt{m_R^2+(g/c_N)^2}}\right)\simeq 0.06, \tag{5.6}$$

which are almost equal to their values in the unperturbed case. Accordingly, one sees that in the region $s\gtrsim 2$ $(GeV/c)^2$ the N-resonances possess the same residue-structure as that of the g=0 case, that is to say, the cross-over phenomenon hardly affects every resonance except two or three states with the small masses. On the other hand, the cross-over phenomenon is extremely important in the prediction of the high-energy backward differential cross-section, because the g=0 case fails to give the dip-structure in π^+p scattering. [See the next section.]

§6. Determination of parameters and prediction as to high-energy backward scattering

In the previous sections, we have seen that the expressions concerning the parent trajectories contain the four adjustable parameters. In this section, we determine the values of these parameters by using the experimental data of the elastic widths of some low-mass states.[13] Then we get the predictions as to the elastic widths of many other resonances and as to forward and backward scattering at high-energy. It is well-known that the dual model generally gives good fits to the near forward cross-section and the fit is stable for such a modification of the baryon trajectories as discussed in this paper. Therefore, we concentrate our attention to the near backward scattering only.

The backward scattering cross-section and polarization are most conveniently expressed in terms of the u-channel parity-definite amplitudes,[12]

$$\tilde{F}_I^{\pm}(\sqrt{u},s)= \mp A_I(u,t,s)+(\sqrt{u}\pm M)B_I(u,t,s), \tag{6.1}$$

for which we get in our model

$$\tilde{F}^{+}_{3/2}(\sqrt{u},s)\simeq -\pi\frac{1-i\exp(-i\pi\alpha_\Delta(\sqrt{u}))}{\Gamma(\alpha_\Delta(\sqrt{u})+\frac{1}{2})\ \sin\pi(\alpha_\Delta(\sqrt{u})-\frac{1}{2})}(bs)^{\alpha_\Delta(\sqrt{u})-\frac{1}{2}}\left\{-x^{\Delta}_{3/2}+(\sqrt{u}+M)\tilde{x}^{\Delta}_{3/2}\right\}, \tag{6.2}$$

$$\tilde{F}^{+}_{1/2}(\sqrt{u},s)\simeq \pi\frac{1+i\exp(-i\pi\alpha^I_N(u))}{\Gamma(\alpha^I_N(u)+\frac{1}{2})\ \sin\pi(\alpha^I_N(u)-\frac{1}{2})}(bs)^{\alpha^I_N(u)-\frac{1}{2}}$$

$$\times\left[\tfrac{1}{2}\left(1+\frac{\sqrt{u}}{\sqrt{u+(g/c_N)^2}}\right)\left\{-x^{N1}_{\frac{1}{2}}+(\sqrt{u}+M)\tilde{x}^{N1}_{\frac{1}{2}}\right\}+\tfrac{1}{2}\left(1-\frac{\sqrt{u}}{\sqrt{u+(g/c_N)^2}}\right)\left\{-x^{N2}_{\frac{1}{2}}+(\sqrt{u}+M)\tilde{x}^{N2}_{\frac{1}{2}}\right\}\right]$$

$$+\pi\frac{1+i\exp(-i\pi\alpha_N^{II}(u))}{\Gamma(\alpha_N^{II}(u)+\frac{1}{2})\sin\pi(\alpha_N^{II}(u)-\frac{1}{2})}(bs)^{\alpha_N^{II}(u)-\frac{1}{2}}$$

$$\times\left[\tfrac{1}{2}\left(1-\frac{\sqrt{u}}{\sqrt{u+(g/c_N)^2}}\right)\left\{-x^{N1}_{\frac{1}{2}}+(\sqrt{u}+M)\widetilde{x^{N1}_{\frac{1}{2}}}\right\}+\tfrac{1}{2}\left(1+\frac{\sqrt{u}}{\sqrt{u+(g/c_N)^2}}\right)\left\{-x^{N2}_{\frac{1}{2}}+(\sqrt{u}+M)\widetilde{x^{N2}_{\frac{1}{2}}}\right\}\right], \tag{6.3}$$

and

$$\widetilde{F^{-}_{I}}(\sqrt{u},s)=-\widetilde{F^{+}_{I}}(-\sqrt{u},s). \tag{6.4}$$

Here the subscript of the $\widetilde{F^{\mp}_{I}}$ represents the u-channel isospin. The u-channel parity-definite amplitudes for given s-channel processes [the l.h.s. of (6.5)] are written as

$$\begin{aligned}
&\widetilde{F^{\pm}}\left[\bar{\pi}p\to\bar{\pi}p\right]=\widetilde{F^{\pm}_{3/2}}\ ,\\
&\widetilde{F^{\pm}}\left[\pi^{+}p\to\pi^{+}p\right]=\tfrac{2}{3}\widetilde{F^{\pm}_{1/2}}+\tfrac{1}{3}\widetilde{F^{\pm}_{3/2}}\ ,\\
&\widetilde{F^{\pm}}\left[\bar{\pi}p\to\pi^{0}n\right]=\tfrac{\sqrt{2}}{3}\left(\widetilde{F^{\pm}_{1/2}}-\widetilde{F^{\pm}_{3/2}}\right)\ ,
\end{aligned} \tag{6.5}$$

and the cross-section and polarization in the near backward region can be obtained from these amplitudes[12]:

$$\frac{d\sigma}{du}\simeq\frac{1}{32\pi s}\left(\left|\widetilde{F^{-}}\right|^2+\left|\widetilde{F^{+}}\right|^2\right),\qquad Po\simeq\frac{\left|\widetilde{F^{-}}\right|^2-\left|\widetilde{F^{+}}\right|^2}{\left|\widetilde{F^{-}}\right|^2+\left|\widetilde{F^{+}}\right|^2}\ . \tag{6.6}$$

(I) Elastic widths of Δ- resonances and near backward $\bar{\pi}p$ elastic scattering at high-energy

The two adjustable parameters, $x^{\Delta}_{3/2}$ and $\widetilde{x^{\Delta}_{3/2}}$ in (6.2), are now determined so that the model reproduces the experimental data for the elastic widths of the two I=3/2 states, $\Gamma^{exp}_{ela}(P_{33};1236)=100\sim120$ MeV and

$\Gamma^{exp}_{ela}(D_{33};1670)=30\sim70$ MeV.[13] Inserting the values $\Gamma_{ela}(P_{33};1236)$ $=100$ MeV and $\Gamma_{ela}(D_{33};1670)=70$ MeV into the expression (4.17), we get

$$x^{\Delta}_{3/2}=101\ \text{GeV}^{-1} \quad \text{and} \quad \widetilde{x^{\Delta}_{3/2}}=103\ \text{GeV}^{-2}. \tag{6.7}$$

The predicted near backward π^-p differential cross-section is shown in Fig. 9. A good agreement with the data[10] is obtained.

Fig. 9

It should be noted that all the previously proposed πN dual models[1] predict too large cross-section for the backward scattering. Our model is distinct from these models at two points: (i) We assume the non-linear trajectories, so that our intercept of the Δ-trajectory is -0.3 but the conventional linear trajectory gives +0.1. (ii) The residue-function of our Δ_γ-Δ_δ trajectory gives at $u\simeq0$ a quite small absolute value than that of the conventional model. Clearly, our lower Δ- intercept leads to small backward cross-section at high-energy. The second point mentioned above is due to the fact that in our model the $P_{33}(1236)$ state has the parity partner $D_{33}(1670)$. In the conventional model with the linear Δ-trajectory, the parity partner of the $P_{33}(1236)$ corresponds to the unobserved state for which we assume the vanishing residue. In Fig. 10 we show this situation; our residue function is given by

$$\gamma_\Delta(\sqrt{u})=-x^{\Delta}_{3/2}+(\sqrt{u}+M)\widetilde{x^{\Delta}_{3/2}}=-4+103\sqrt{u}\ , \tag{6.8}$$

but the conventional one by

$$\gamma_\Delta(\sqrt{u})=-66+53\sqrt{u}\ , \tag{6.9}$$

which vanishes at $\sqrt{u}=1.236$ GeV/c. Our residue-function gives the smaller absolute value at u=0, which is preferable for obtaining the small backward cross-section.

Fig. 10

In the model with the linear Δ-trajectory, the wrong signature nonsense zero occurs at $u\simeq -1.7$ $(\mathrm{GeV}/c)^2$, i.e., $\alpha_\Delta(u)=-3/2$. However, the expected dip-structure is not seen experimentally [see Fig. 9]. In our case, the trajectory-function $\alpha_\Delta(\sqrt{u})$ becomes complex for $u<0$; no dip appears there and good fits are obtained for the experimental values.

(II) Elastic widths of N-resonances and near backward $\pi^+ p$ elastic and $\pi^- p$ charge-exchange scattering at high-energy

As seen in (5.3) and (5.4), the elastic widths of N-resonances depend on the four parameters, $x_{\frac{1}{2}}^{N1}$, $\widetilde{x_{\frac{1}{2}}^{N1}}$, $x_{\frac{1}{2}}^{N2}$ and $\widetilde{x_{\frac{1}{2}}^{N2}}$, but owing to the restrictions (4.12) we have only two adjustable ones. In order to determine the values of these parameters, we now use the experimental nucleon coupling constants, $g_{\pi NN}^2/4\pi\simeq 14$, and the requirement of the elimination of the $S_{11}(939)$, i.e., the parity partner of the nucleon predicted by the perturbed trajectory. Thus, it is obtained that

$$\frac{1}{12\pi bM}\left[\tfrac{1}{2}\left(1+\frac{M}{\sqrt{M^2+(g/c_N)^2}}\right)\left(-x_{\frac{1}{2}}^{N1}+2M\widetilde{x_{\frac{1}{2}}^{N1}}\right)+\tfrac{1}{2}\left(1-\frac{M}{\sqrt{M^2+(g/c_N)^2}}\right)\left(-x_{\frac{1}{2}}^{N2}+2M\widetilde{x_{\frac{1}{2}}^{N2}}\right)\right]=14,$$

$$\tfrac{1}{2}\left(1-\frac{M}{\sqrt{M^2+(g/c_N)^2}}\right)x_{\frac{1}{2}}^{N1}+\tfrac{1}{2}\left(1+\frac{M}{\sqrt{M^2+(g/c_N)^2}}\right)x_{\frac{1}{2}}^{N2}=0\ ,$$

$$x_{\frac{1}{2}}^{N1}+x_{\frac{1}{2}}^{N2}=-x_{3/2}^{\Delta}=-101\ \mathrm{GeV}^{-1},$$

$$\widetilde{x_{\frac{1}{2}}^{N1}}+\widetilde{x_{\frac{1}{2}}^{N2}}=2\widetilde{x_{3/2}^{\Delta}}=206\ \mathrm{GeV}^{-2}, \qquad (6.10)$$

which lead to

$$x_{\frac{1}{2}}^{N1}=-116\ \mathrm{GeV}^{-1},\ \widetilde{x_{\frac{1}{2}}^{N1}}=195\ \mathrm{GeV}^{-2},\ x_{\frac{1}{2}}^{N2}=15\ \mathrm{GeV}^{-1}\ \text{and}\ \widetilde{x_{\frac{1}{2}}^{N2}}=11\ \mathrm{GeV}^{-2}. \qquad (6.11)$$

By using the values of (6.11) we can predict the elastic widths of the other well-established N-resonances. The results are shown in Table 1.

We next give the results of our calculation on $\pi^+ p$ elastic and $\pi^- p$ charge-exchange backward cross-sections.[10] [Fig.11]

Fig. 11

As seen in Fig.11, we get the fairly good results for the $\pi^+ p$ elastic differential cross-section in the backward region ($u < -0.05$ $(GeV/c)^2$) except for very near $\theta = 180^\circ$. The fit to charge-exchange scattering is less successful. At $u \simeq 0$ $(GeV/c)^2$, the predicted cross-sections for both the cases are larger than the experimental values, by a factor of two or three. However the improvement of the backward cross-sections are very remarkable; the previous models predict about 100 times of the experimental values.

Our model gives the well-known dip-structure due to the wrong signature nonsense zero at $\alpha_N^I(-0.15) = -1/2$. The cross-over phenomenon plays an essential role for this fact, because the wrong signature nonsense point of the unperturbed trajectory appears at $u \simeq 0.08$ $(GeV/c)^2$ [see Fig. 4].

The result of our calculation on $\pi^+ p$ polarization[14] is shown in Fig. 12.

Fig. 12

As seen in Fig.12, we get the good result in the region $u < -0.2$ $(GeV/c)^2$. At $u \simeq 0$ and -0.15 $(GeV/c)^2$, the predicted values are larger than the experimental ones, by a factor of two or three. The dip and bump structure in the region $u > -0.3$ $(GeV/c)^2$ is mainly due to the interference between the contributions from the N- and Δ- trajectories. On the other hand, in the region $u < -0.3$ $(GeV/c)^2$ the dominant contribution comes from the N-trajectories whose contribution is large and negative.

§7. Concluding remarks

In the previous sections, we have seen that many difficulties so far encountered in the Veneziano model with linear baryon trajectories are overcome by assuming the non-linear baryon trajectories for which the cross-over phenomenon is taken into account. The three (s,t and u) channels in πN scattering are all non-exotic. The duality, therefore, imposes stronger restrictions on the amplitude than the case of the KN scattering where one of the channels is exotic. So far many difficulties mentioned before have prevented to see whether the duality is actually valid or not in this most interesting case. However, our result clearly shows that the duality is a good working hypothesis even for the case of the strongest restrictions (i.e., πN scattering). This is very encouraging situation.

We have not discussed so much the near forward cross-sections. These are controlled by the meson trajectories and thus our model gives the similar results to the previous models, where we have already had successful results.

We have not also discussed the property of our amplitude at the Adler point and the values of the scattering length. These depend on the multiplicative constants which are connected with the daughter trajectories and have been yet undetermined; eight constants still remain. We have sufficient freedom of the low-energy amplitude.

Acknowledgements

I would like to express my sincere gratitude to Prof. R. Utiyama for his continual encouragement and for kind hospitality. I would like to thank Prof. T. Kanki for useful conversations and for reading of the manuscript.

Appendix

We shall show that the expression (3.10) is derived from the following integral representation (3.11):

$$xB(\tfrac{1}{2}-\alpha_s, 1-\alpha_M(t))+\tilde{x}\tilde{B}(\tfrac{1}{2}-\alpha_s, 1-\alpha_M(t))$$
$$= \tfrac{1}{2}\int_0^1 dw\ w^{-\alpha_s-\frac{1}{2}}(x+\tilde{x}\alpha_1)(1-w)^{-\alpha_M(t)}$$
$$+\tfrac{1}{2}\int_0^1 dw\ w^{-\alpha_M(t)}(x+\tilde{x}\alpha_2)(1-w)^{-\alpha_s-\frac{1}{2}} . \qquad (A.1)$$

This representation is multiplied by the identity,

$$\frac{\sqrt{s}-\not{p}_s}{2\sqrt{s}} + \frac{\sqrt{s}+\not{p}_s}{2\sqrt{s}} = 1 , \qquad (A.2)$$

and using the eigenvalue equations,

$$(\sqrt{s}\mp\not{p}_s)(\not{\alpha}_s)^n = (\not{\alpha}_s)^n(\sqrt{s}\mp\not{p}_s) = (\sqrt{s}\mp\not{p}_s)(\not{\alpha}(\pm\sqrt{s}))^n , \qquad (A.3)$$

we get for (A.1)

$$\left[\frac{\sqrt{s}-\not{p}_s}{2\sqrt{s}} + \frac{\sqrt{s}+\not{p}_s}{2\sqrt{s}}\right]\left\{\tfrac{1}{2}\int_0^1 dw\ w^{-\alpha_s-\frac{1}{2}}(x+\tilde{x}\alpha_1)(1-w)^{-\alpha_M(t)}\right\}$$
$$+\left\{\tfrac{1}{2}\int_0^1 dw\ w^{-\alpha_M(t)}(x+\tilde{x}\alpha_2)(1-w)^{-\alpha_s-\frac{1}{2}}\right\}\left[\frac{\sqrt{s}-\not{p}_s}{2\sqrt{s}} + \frac{\sqrt{s}+\not{p}_s}{2\sqrt{s}}\right]$$
$$= \left[\frac{\sqrt{s}-\not{p}_s}{4\sqrt{s}}(x+\tilde{x}\alpha_1) + (x+\tilde{x}\alpha_2)\frac{\sqrt{s}-\not{p}_s}{4\sqrt{s}}\right]\left\{\int_0^1 dw\ w^{-\alpha(\sqrt{s})-\frac{1}{2}}(1-w)^{-\alpha_M(t)}\right\}$$
$$+\left[\frac{\sqrt{s}+\not{p}_s}{4\sqrt{s}}(x+\tilde{x}\alpha_1) + (x+\tilde{x}\alpha_2)\frac{\sqrt{s}+\not{p}_s}{4\sqrt{s}}\right]\left\{\int_0^1 dw\ w^{-\alpha(-\sqrt{s})-\frac{1}{2}}(1-w)^{-\alpha_M(t)}\right\}. \qquad (A.4)$$

The integral representations are factorized from the matrices and they give the beta-functions in (3.10). One can see that the matrices in (A.4) are equal to the matrices in (3.10), respectively, because

we have the following identities when the matrices are inserted between the Dirac spinors:

$$\bar{u}(p_2)\not{p}_s u(p_1)=\bar{u}(p_2)[M+\not{q}]u(p_1),$$

$$\bar{u}(p_2)\not{q}_1 u(p_1)=\bar{u}(p_2)\not{q}_2 u(p_1)=\bar{u}(p_2)\not{q}u(p_1)$$

$$\bar{u}(p_2)\not{p}_s\not{q}_1 u(p_1)=\bar{u}(p_2)\not{q}_2\not{p}_s u(p_1)=\bar{u}(p_2)[s-M^2-M\not{q}]u(p_1). \qquad (A.5)$$

Q. E. D.

The (t-u) term and the (s-u) term are obtained by the same technique:

$$B(1-\alpha_M(t),\tfrac{1}{2}-\alpha'_u)$$

$$= \frac{\sqrt{u}-M+\not{q}}{2\sqrt{u}}B(1-\alpha_M(t),\tfrac{1}{2}-\alpha(\sqrt{u})) + \frac{\sqrt{u}+M-\not{q}}{2\sqrt{u}}B(1-\alpha_M(t),\tfrac{1}{2}-\alpha(-\sqrt{u})), \qquad (A.6)$$

$$\tilde{B}(1-\alpha_M(t),\tfrac{1}{2}-\alpha'_u)$$

$$= \frac{u-M^2+(\sqrt{u}+M)\not{q}}{2\sqrt{u}}B(1-\alpha_M(t),\tfrac{1}{2}-\alpha(\sqrt{u})) + \frac{-u+M^2+(\sqrt{u}-M)\not{q}}{2\sqrt{u}}B(1-\alpha_M(t),\tfrac{1}{2}-\alpha(-\sqrt{u})), \qquad (A.7)$$

$$B(\tfrac{1}{2}-\alpha'_s,\tfrac{1}{2}-\alpha'_u)$$

$$= \frac{1}{4\sqrt{su}}\left[-M(\sqrt{s}+\sqrt{u})+\sqrt{su}+(M^2-\mu^2)+\not{q}(\sqrt{s}-\sqrt{u})\right]B(\tfrac{1}{2}-\alpha(\sqrt{s}),\tfrac{1}{2}-\alpha(\sqrt{u}))$$

$$+ \frac{1}{4\sqrt{su}}\left[M(\sqrt{s}-\sqrt{u})+\sqrt{su}-(M^2-\mu^2)-\not{q}(\sqrt{s}+\sqrt{u})\right]B(\tfrac{1}{2}-\alpha(\sqrt{s}),\tfrac{1}{2}-\alpha(-\sqrt{u}))$$

$$+ \frac{1}{4\sqrt{su}}\left[-M(\sqrt{s}-\sqrt{u})+\sqrt{su}-(M^2-\mu^2)+\not{q}(\sqrt{s}+\sqrt{u})\right]B(\tfrac{1}{2}-\alpha(-\sqrt{s}),\tfrac{1}{2}-\alpha(\sqrt{u}))$$

$$+ \frac{1}{4\sqrt{su}}\left[M(\sqrt{s}+\sqrt{u})+\sqrt{su}+(M^2-\mu^2)-\not{q}(\sqrt{s}-\sqrt{u})\right]B(\tfrac{1}{2}-\alpha(-\sqrt{s}),\tfrac{1}{2}-\alpha(-\sqrt{u})), \qquad (A.8)$$

$$\tilde{B}(\tfrac{1}{2}-\alpha'_s,\tfrac{1}{2}-\alpha'_u)$$

$$= \frac{1}{4\sqrt{su}}\Big[\, M(s-u)-(s\sqrt{u}-u\sqrt{s})-M^2(\sqrt{s}-\sqrt{u})+\not{\alpha}\{-(s+u)+\sqrt{su}+M(\sqrt{s}+\sqrt{u})-(M^2-\mu^2)\}\Big]$$

$$\times B(\tfrac{1}{2}-\alpha(\sqrt{s}),\tfrac{1}{2}-\alpha(\sqrt{u}))$$

$$+\frac{1}{4\sqrt{su}}\Big[-M(s-u)-(s\sqrt{u}+u\sqrt{s})+M^2(\sqrt{s}+\sqrt{u})+\not{\alpha}\{(s+u)+\sqrt{su}-M(\sqrt{s}-\sqrt{u})+(M^2-\mu^2)\}\Big]$$

$$\times B(\tfrac{1}{2}-\alpha(\sqrt{s}),\tfrac{1}{2}-\alpha(-\sqrt{u}))$$

$$+\frac{1}{4\sqrt{su}}\Big[-M(s-u)+(s\sqrt{u}+u\sqrt{s})-M^2(\sqrt{s}+\sqrt{u})+\not{\alpha}\{(s+u)+\sqrt{su}+M(\sqrt{s}-\sqrt{u})+(M^2-\mu^2)\}\Big]$$

$$\times B(\tfrac{1}{2}-\alpha(-\sqrt{s}),\tfrac{1}{2}-\alpha(\sqrt{u}))$$

$$+\frac{1}{4\sqrt{su}}\Big[\, M(s-u)+(s\sqrt{u}-u\sqrt{s})+M^2(\sqrt{s}-\sqrt{u})+\not{\alpha}\{-(s+u)+\sqrt{su}-M(\sqrt{s}+\sqrt{u})-(M^2-\mu^2)\}\Big]$$

$$\times B(\tfrac{1}{2}-\alpha(-\sqrt{s}),\tfrac{1}{2}-\alpha(-\sqrt{u})), \qquad \text{(A.9)}$$

where μ denotes the pion mass.

References

1) K. Igi, Phys. Letters 28B (1968), 330.
Y. Hara, Phys. Rev. 182 (1969), 1906.
S. K. Bose and K. C. Gupta, Phys. Rev. 184 (1969), 1572.
M. A. Virasoro, Phys. Rev. 184 (1969), 1621.
J. Namysiowski, Nuovo Cim. 64A (1969), 555.
E. L. Berger and G. C. Fox, Phys. Rev. 188 (1969), 2120.
A. Garcia and L. Masperi, Lett. Nuovo Cim. 4 (1970), 929.
S. Fenster and K. C. Wali, Phys. Rev. D1 (1970), 1409.
G. C. Joshi and A. Pagnamenta, Phys. Rev. D1 (1970), 3117.
K. Hirose and T. Kanki, Prog. Theor. Phys. 47 (1972), 184.

2) S. W. MacDowell, Phys. Rev. 116 (1959), 774.
V. N. Gribov, JETP 43 (1962), 1529 Sov. Phys. 16 (1963), 1080.
T. Kanki, G. Konisi and T. Saito, Prog. Theor. Phys. 40 (1968), 394.

3) V. Barger and D. Cline, Phys. Rev. Letters 20 (1968), 298.

4) D. Sivers, Phys. Rev. D4 (1971), 1944.
M. Ida, Lett. Nuovo Cim. 4 (1972), 707; Prog. Theor. Phys. 48 (1972), 2346.
K. Hirose, Prog. Theor. Phys. 51 (1974), 823.

5) D. E. Plane et al., Nucl. Phys. B22 (1970), 93.

6) A.Ahmadzadeh, P. G. Burke and C. Tate, Phys. Rev. 131 (1963), 1315.
M. Ida, Prog. Theor. Phys. 49 (1973), 1259.

7) R. Gatto and P. Menotti, Nuovo Cim. 68A (1970), 118.
N. Murai, K. Nakamura and H. Ezawa, Prog. Theor. Phys. 46 (1971), 909.

8) V. N. Gribov, Soviet Phys. JETP 26 (1968), 414.

9) D. V. Volkov and V. V. Radchenko. Phys. Letters 36B (1971), 83.

10) D. P. Owen et al. Phys. Rev. 181 (1969), 1794.
J. P. Boright et al. Phys. Letters 33B (1970), 615.
11) C. B. Chiu and J. D. Stack, Phys. Rev. 153 (1967), 1575.
E. L. Berger and G. C. Fox, Nucl. Phys. B26 (1971), 1.
12) V. Barger and C. Cline, Phenomenological Theories of High-Energy Scattering (Benjamin, New York, 1969), Chaps. 3 and 7.
13) Resonance data are taken from Particle Data Groups, Rev. Mod. Phys. 45 (1973), No.2, Part II.
14) L. Dick et al., Nucl. Phys. B43 (1972), 522.

Figure Captions

Fig. 1. The Δ_γ-Δ_δ trajectory.

Fig. 2. The Chew-Frautschi plot of the Δ_γ-Δ_δ trajectory.

Fig. 3. The unperturbed N trajectories.

Fig. 4. The Chew-Frautschi plot of the unperturbed N trajectories.

Fig. 5. The cross-over phenomenon between the N_α-N'_β and N'_α -N_β trajectories.

Fig. 6. The Reggeon diagrams which produce the cross-over phenomenon.

Fig. 7. Two branch points of the perturbed trajectory-function and the cuts extending from them.

Fig. 8. The Chew-Frautschi plot of the perturbed N trajectories.

Fig. 9. The near backward differential cross-section in π^-p elastic scattering.

Fig.10. The residue function of the Δ trajectories.

Fig.11. The near backward differential cross-sections in π^+p elastic and π^-p charge-exchange scattering.

Fig.12. The near backward polarization in π^+p elastic scattering at 6 GeV/c incident pion momentum.

Table 1. The prediction of the elastic widths.

	Γ^{theo}_{ela} (MeV)	Γ^{exp}_{ela} (MeV)
$P_{11}(1470)$	81	90∼140
$S_{11}(1535)$	50	13∼50
$D_{15}(1670)$	32	43∼68
$F_{15}(1688)$	42	56∼'99

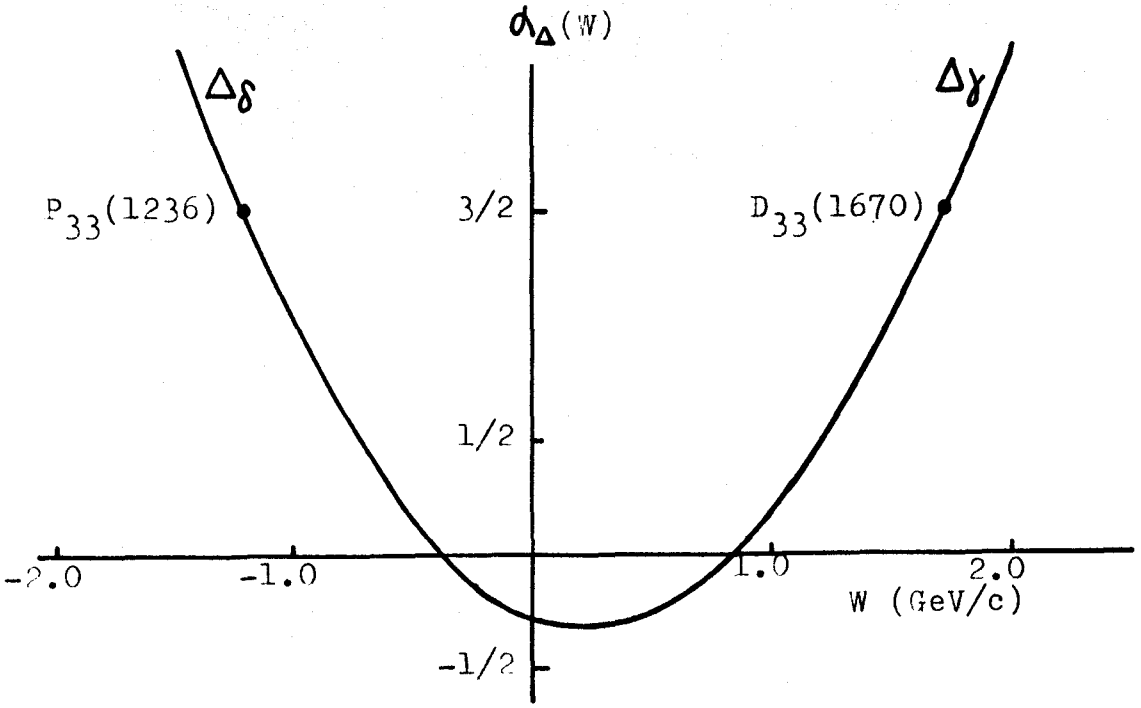
$\alpha_\Delta(W)$
Δ_δ
Δ_γ
$P_{33}(1236)$
$D_{33}(1670)$
3/2
1/2
-1/2
-2.0
-1.0
1.0
2.0
W (GeV/c)

Fig. 1

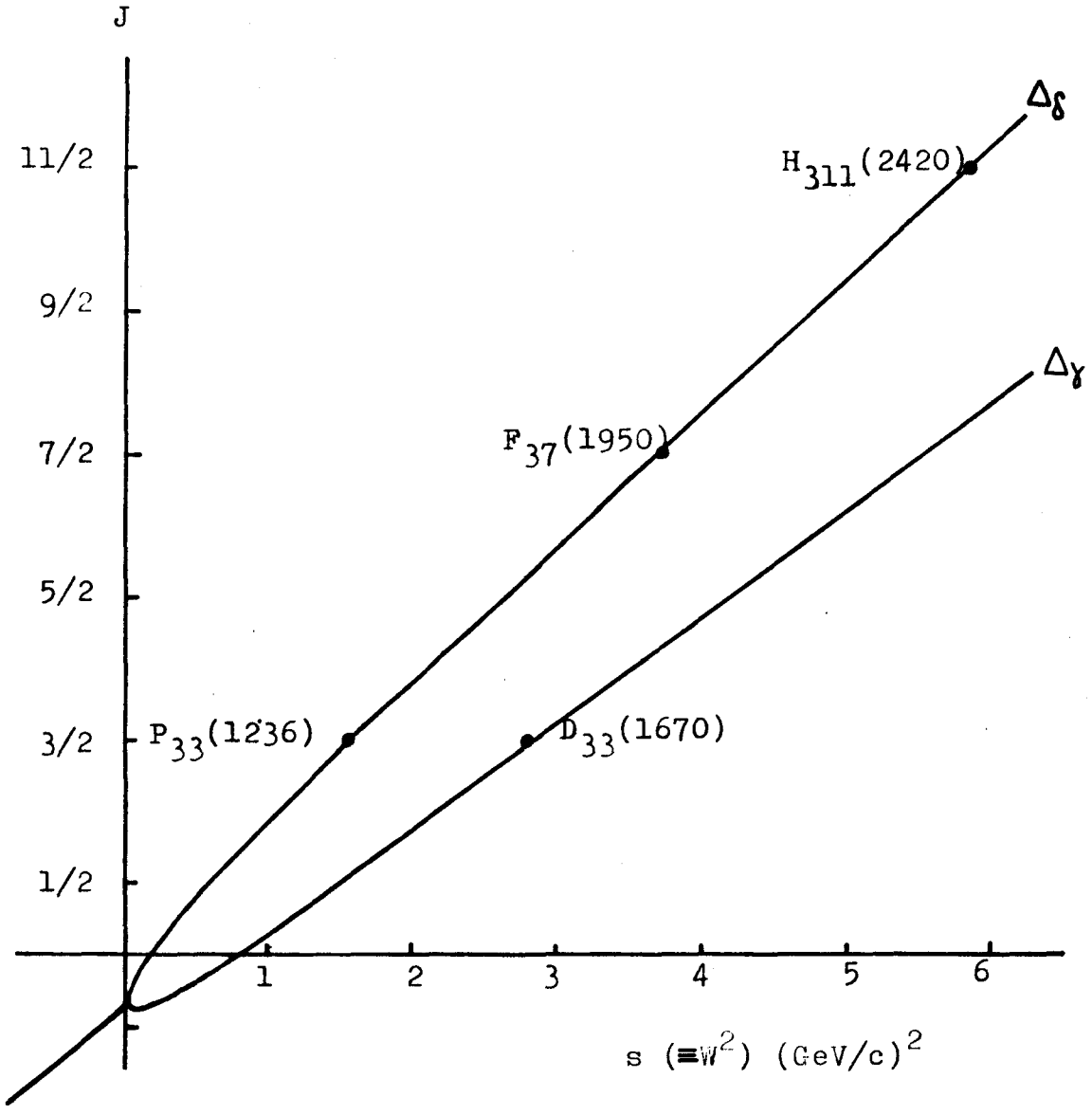
J
11/2
9/2
7/2
5/2
3/2
1/2
Δ_δ
Δ_γ
$H_{311}(2420)$
$F_{37}(1950)$
$P_{33}(1236)$
$D_{33}(1670)$
1
2
3
4
5
6
s ($\equiv W^2$) (GeV/c)^2

Fig. 2

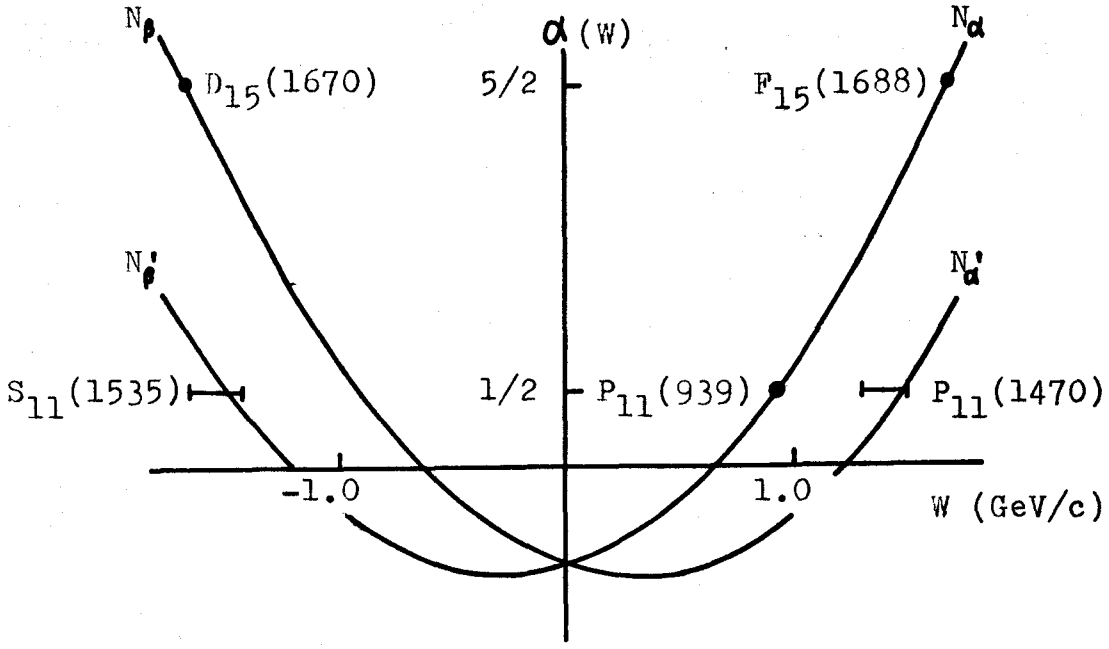
N_β
$D_{15}(1670)$
α (W)
5/2
N_α
$F_{15}(1688)$
N'_β
N'_α
$S_{11}(1535)$
1/2
$P_{11}(939)$
$P_{11}(1470)$
-1.0
1.0
W (GeV/c)

Fig. 3

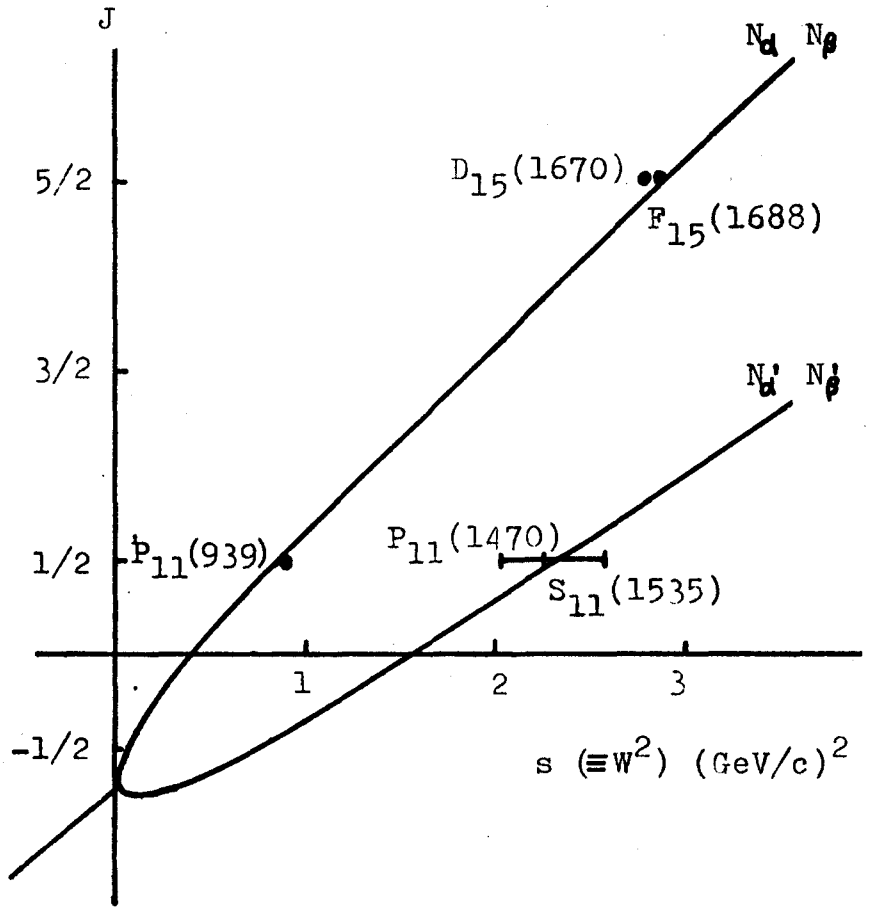
J
N_α N_β
5/2
$D_{15}(1670)$
$F_{15}(1688)$
3/2
N'_α N'_β
1/2
$P_{11}(939)$
$P_{11}(1470)$
$S_{11}(1535)$
1
2
3
-1/2
s ($\equiv W^2$) (GeV/c)^2

Fig. 4

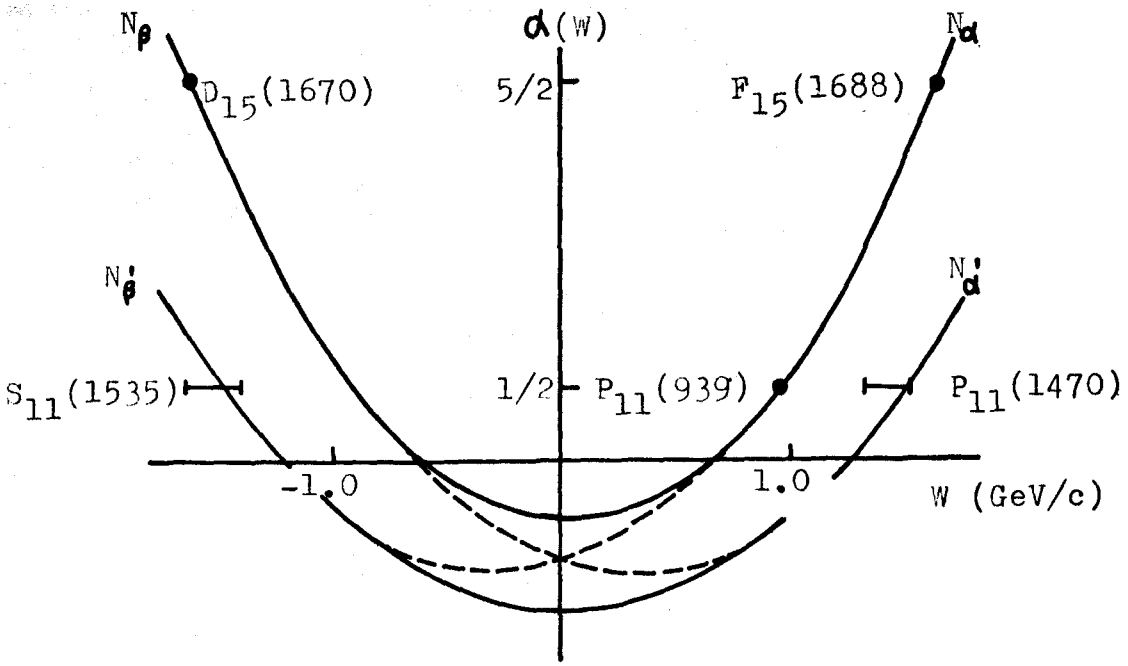

Fig. 5

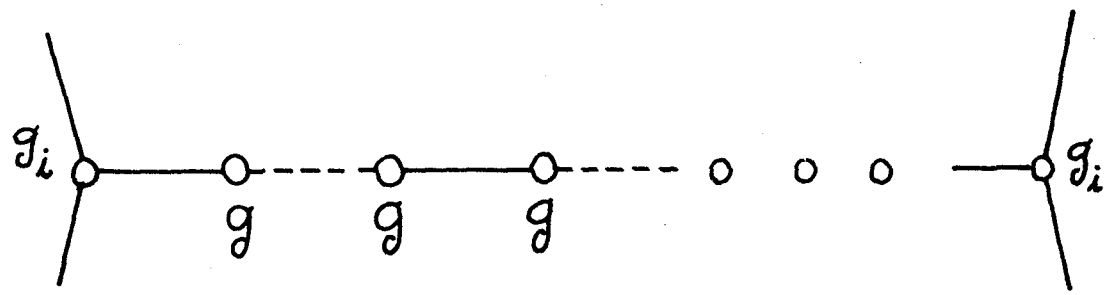

Fig. 6

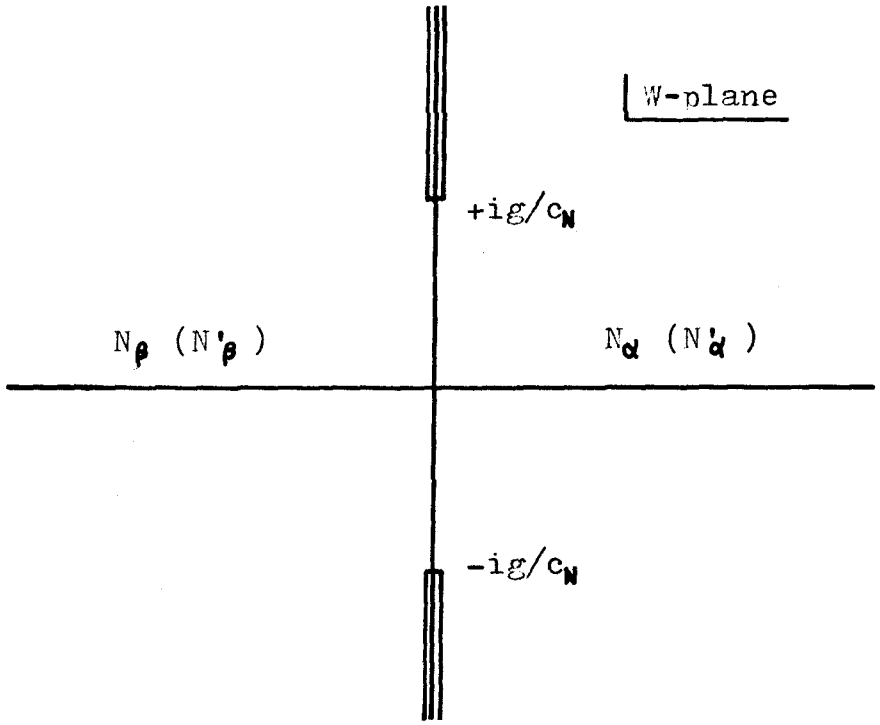

Fig. 7

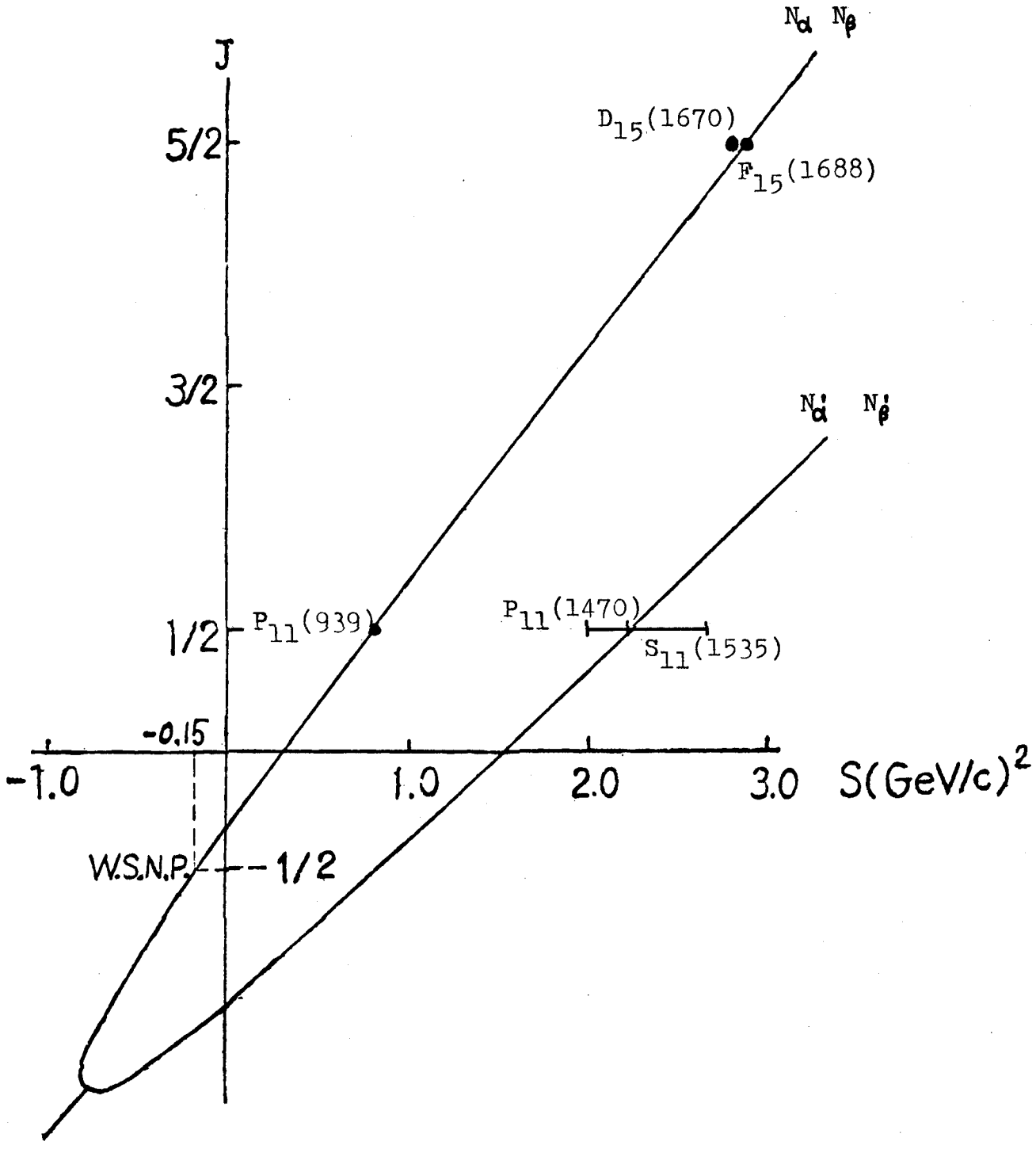
J
5/2
3/2
1/2
N_α N_β
$D_{15}(1670)$
$F_{15}(1688)$
N'_α N'_β
$P_{11}(939)$
$P_{11}(1470)$
$S_{11}(1535)$
-0.15
-1.0
1.0
2.0
3.0
S(GeV/c)^2
W.S.N.P.
1/2

Fig. 8

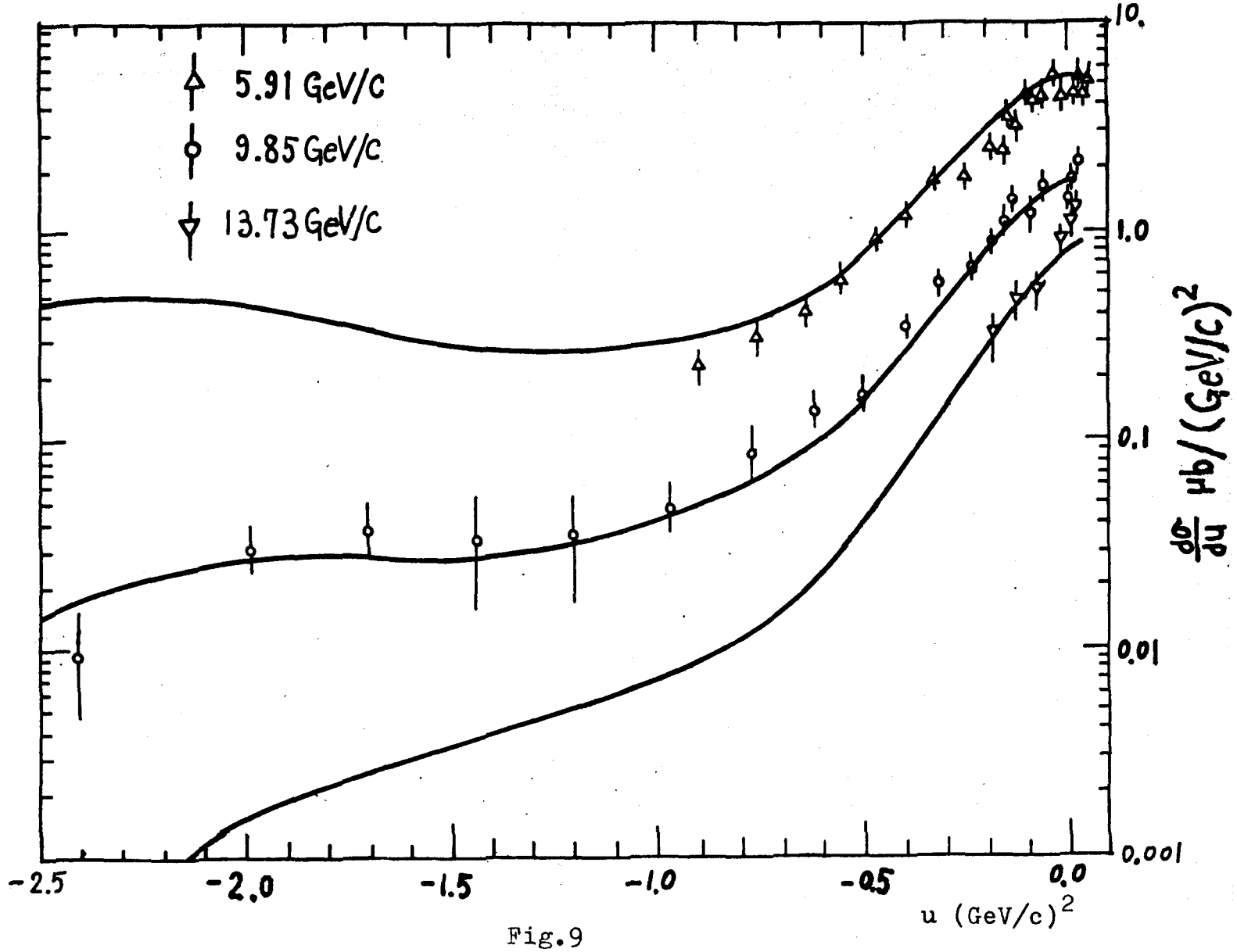
5.91 GeV/c
9.85 GeV/c
13.73 GeV/c
10.
1.0
0.1
0.01
0.001
$\frac{d\sigma}{du}$ μb/(GeV/c)^2
-2.5
-2.0
-1.5
-1.0
-0.5
0.0
u (GeV/c)^2

Fig.9

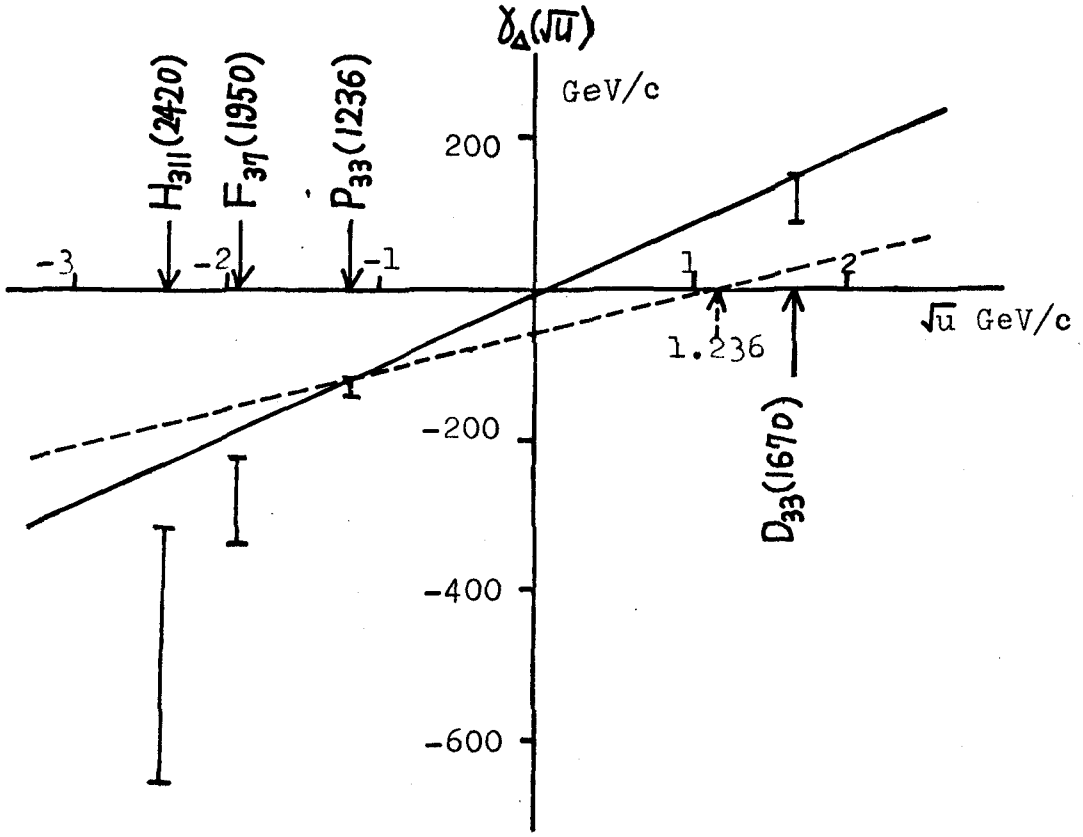
$\gamma_\Delta(\sqrt{u})$
GeV/c
200
-200
-400
-600
$H_{311}(2420)$
$F_{37}(1950)$
$P_{33}(1236)$
$D_{33}(1670)$
-3
-2
-1
1
2
1.236
$\sqrt{u}$ GeV/c

Fig. 10

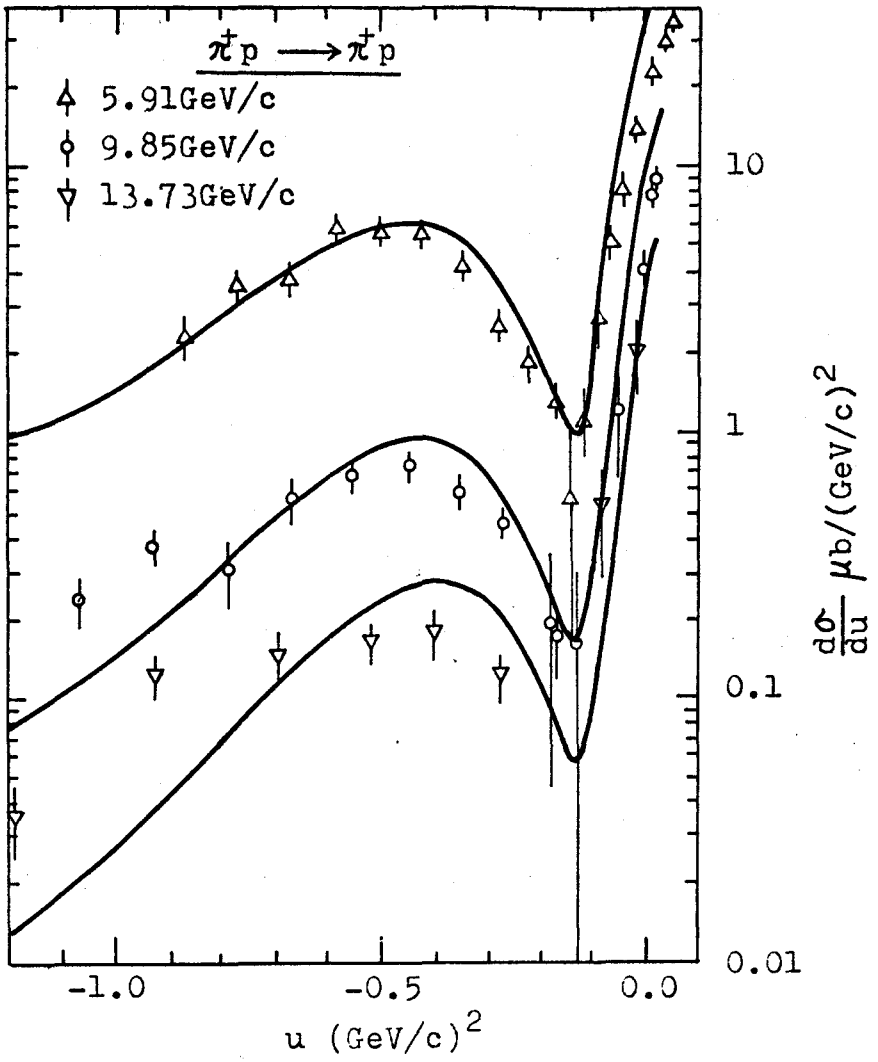
$\pi^+ p \longrightarrow \pi^+ p$
5.91GeV/c
9.85GeV/c
13.73GeV/c
10
1
0.1
0.01
-1.0
-0.5
0.0
u (GeV/c)^2
$\frac{d\sigma}{du}$ μb/(GeV/c)^2

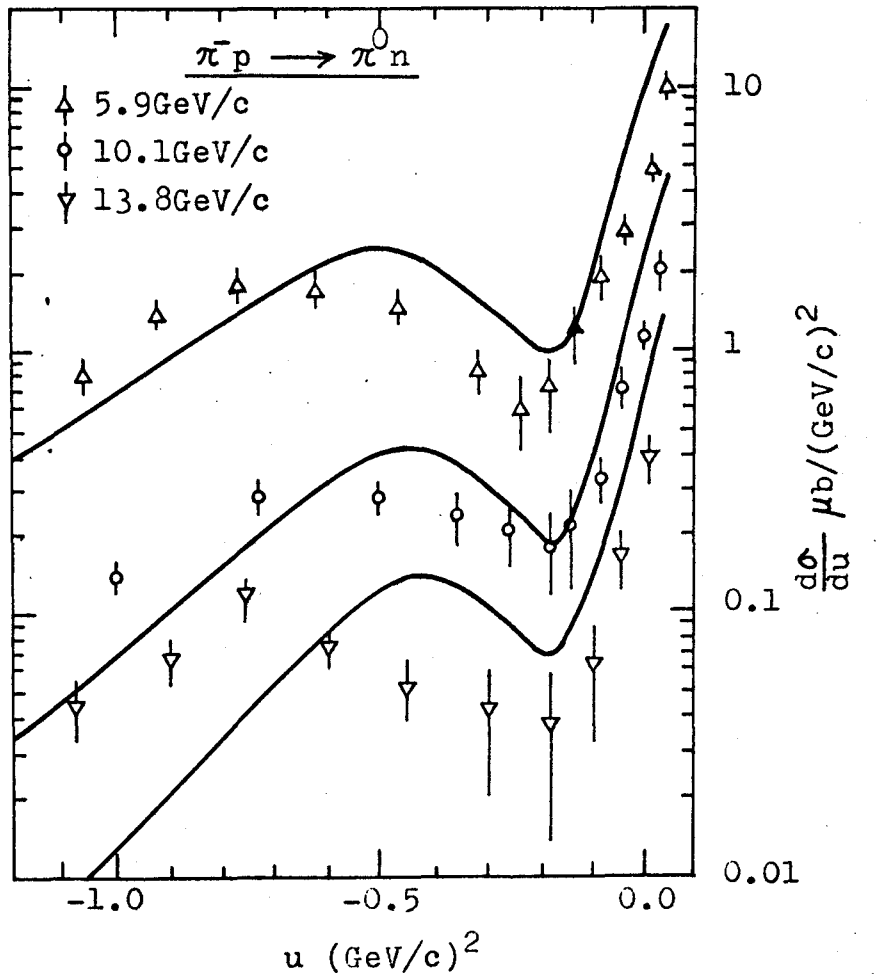
$\pi^- p \longrightarrow \pi^0 n$
5.9GeV/c
10.1GeV/c
13.8GeV/c
10
1
0.1
0.01
-1.0
-0.5
0.0
u (GeV/c)^2
$\frac{d\sigma}{du}$ μb/(GeV/c)^2

Fig. 11

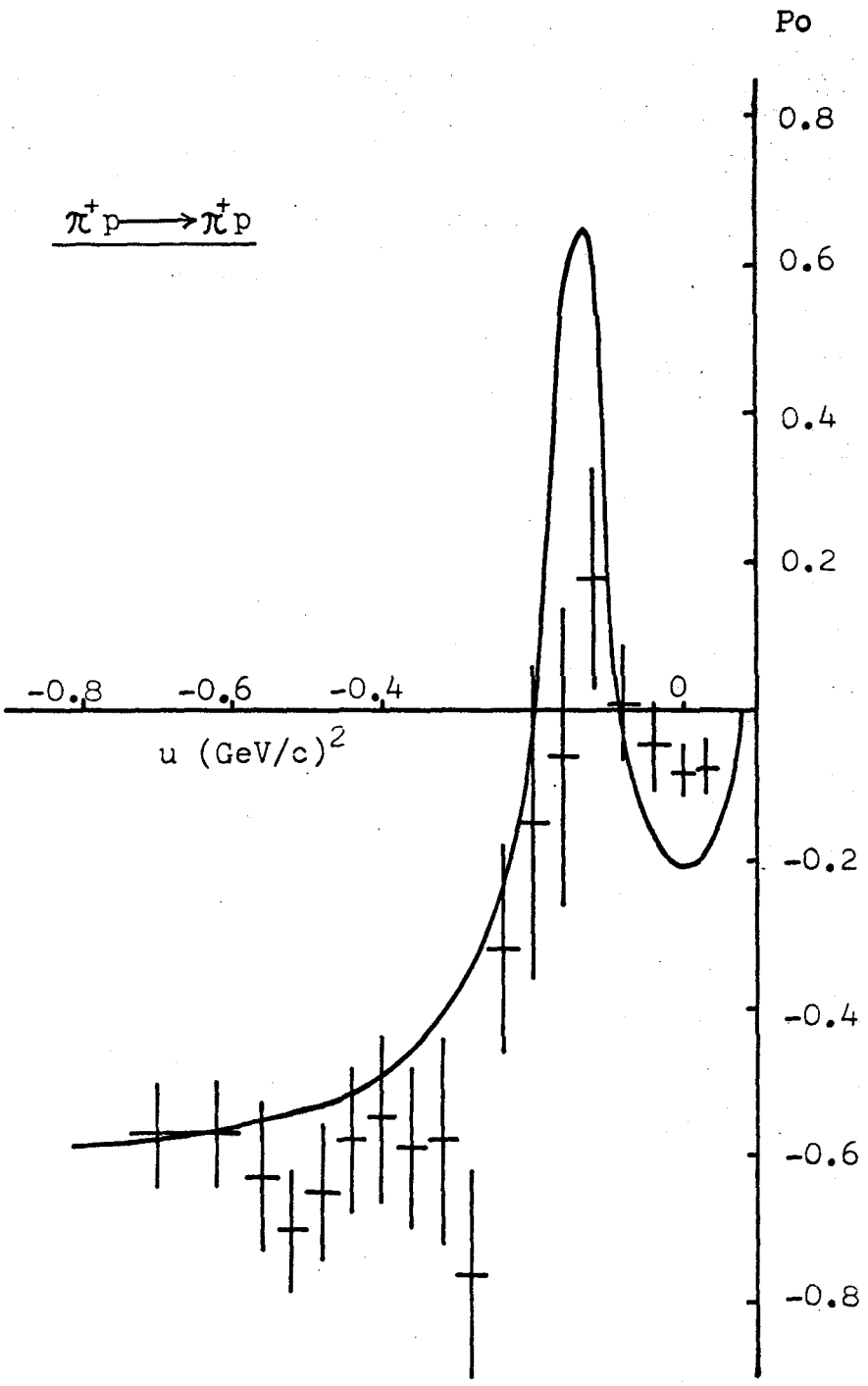
Po
0.8
0.6
0.4
0.2
-0.2
-0.4
-0.6
-0.8
$\pi^+ p \longrightarrow \pi^+ p$
-0.8
-0.6
-0.4
0
u (GeV/c)^2

Fig. 12